hybrid detector showed markedly high performance (72.2% sensitivity, 87.7% specificity, 84.6% accuracy) and a Youden's index of approximately 0.6 for the detection of small HCC. The high accuracy of our hybrid detector in the present blinded, multi-institutional setting is thus fascinating from the perspective of screening for heterogeneous samples within or among various institutes.

We found that AFP test plus $40 resulted in increases of 15.8% and 14.4% of specificity and diagnostic accuracy, respectively. However, the cost-effectiveness of the hybrid detector in surveillance setting remains unclear; further studies are needed to clarify whether the hybrid detector we built could serve as a non-invasive and easy-to-use tool in surveillance programs for HCV-related HCC in the near future.

Acknowledgements

The authors are grateful to Stark Markus PhD, Nozomi Fujita and Hiromi Kaburagi at Roche Diagnostics K.K. for assistance of measurement of methylated DNA amounts in sera from patients, and to Dr. Brian Rhees at Roche Molecular Systems, Inc. for critical suggestions on statistical analysis Grant sponsors: the Ministry of Education, Culture, Sports, Science and Technology (No. 18390366, No. 17591406 and Knowledge Cluster Initiative); the Venture Business Laboratory of Yamaguchi University; the New Energy and Industrial Technology Development Organization (Grant number: 03A02018a).

Appendix A. Supplementary data

Supplementary data to this article can be found online at doi:10.1016/j.cca.2010.09.028.

References

[1] Deuffic S, Poynard T, Buffat L, Valleron AJ. Trends in primary liver cancer. Lancet 1998;351:214–5.
[2] El-Serag HB, Mason AC. Rising incidence of hepatocellular carcinoma in the United States. N Engl J Med 1999;340:745–50.
[3] Parkin DM, Bray F, Ferlay J, Pisani P. Estimating the world cancer burden: Globocan 2000. Int J Cancer 2001;94:153–6.
[4] Bruix J, Sherman M. Practice Guidelines Committee, American Association for the Study of Liver Diseases. Management of hepatocellular carcinoma. Hepatology 2005;42:1208–36.
[5] Llovet JM, Burroughs A, Bruix J. Hepatocellular carcinoma. Lancet 2003;362: 1907–17.
[6] Poynard T, Yuen MF, Ratziu V, Lai CL. Viral hepatitis C. Lancet 2003;362:2095–100.
[7] Bruix J, Sherman M, Llovet JM, Beaugrand M, Lencioni R, Burroughs AK, et al. Clinical management of hepatocellular carcinoma. Conclusions of the Barcelona-2000 EASL conference. European Association for the Study of the Liver. J Hepatol 2001;35:421–30.
[8] Gupta S, Bent S, Kohlwes J. Test characteristics of alpha-fetoprotein for detecting hepatocellular carcinoma in patients with hepatitis C. A systematic review and critical analysis. Ann Intern Med 2003;139:46–50.
[9] El-Serag HB, Marrero JA, Rudolph L, Reddy KR. Diagnosis and treatment of hepatocellular carcinoma. Gastroenterology 2008;134:1752–63.
[10] Herman JG, Baylin SB. Gene silencing in cancer in association with promoter hypermethylation. N Engl J Med 2003;349:2042–54.
[11] Kanai Y, Hui AM, Sun L, Ushijima S, Sakamoto M, Tsuda H, et al. DNA hypermethylation at the D17S5 locus and reduced HIC-1 mRNA expression are associated with hepatocarcinogenesis. Hepatology 1999;29:703–9.
[12] Yoshikawa H, Matsubara K, Qian GS, Jackson P, Groopman JD, Manning JE, et al. SOCS-1, a negative regulator of the JAK/STAT pathway, is silenced by methylation in human hepatocellular carcinoma and shows growth-suppression activity. Nat Genet 2001;28:29–35.
[13] Fukai K, Yokosuka O, Chiba T, Hirasawa Y, Tada M, Imazeki F, et al. Hepatocyte growth factor activator inhibitor 2/placental bikunin (HAI-2/PB) gene is frequently hypermethylated in human hepatocellular carcinoma. Cancer Res 2003;63:8674–9.
[14] Zhang YJ, Wu HC, Shen J, Ahsan H, Tsai WY, Yang HI, et al. Predicting hepatocellular carcinoma by detection of aberrant promoter methylation in serum DNA. Clin Cancer Res 2007;13:2378–84.
[15] Wong IH, Zhang J, Lai PB, Lau WY, Lo YM. Quantitative analysis of tumor-derived methylated p16INK4a sequences in plasma, serum, and blood cells of hepatocellular carcinoma patients. Clin Cancer Res 2003;9:1047–52.
[16] Moribe T, Iizuka N, Miura T, Stark M, Tamatsukuri S, Ishitsuka H, et al. Identification of novel aberrant methylation of BASP1 and SRD5A2 for early diagnosis of hepatocellular carcinoma by genome-wide search. Int J Oncol 2008;33:949–58.
[17] Moribe T, Iizuka N, Miura T, Kimura N, Tamatsukuri S, Ishitsuka H, et al. Methylation of multiple genes as molecular markers for diagnosis of a small, well-differentiated hepatocellular carcinoma. Int J Cancer 2009;125:388–97.
[18] Dupuy A, Simon RM. Critical review of published microarray studies for cancer outcome and guidelines on statistical analysis and reporting. J Natl Cancer Inst 2007;99:147–57.
[19] Iizuka N, Oka M, Yamada-Okabe H, Nishida M, Maeda Y, Mori N, et al. Oligonucleotide microarray for prediction of early intrahepatic recurrence of hepatocellular carcinoma after curative resection. Lancet 2003;361:923–9.
[20] Ikai I, Takayasu K, Omata M, Okita K, Nakanuma Y, Matsuyama Y, et al. Liver Cancer Study Group of Japan. A modified Japan Integrated Stage score for prognostic assessment in patients with hepatocellular carcinoma. J Gastroenterol 2006;41:884–92.
[21] Giannelli G, Antonaci S. New frontiers in biomarkers for hepatocellular carcinoma. Dig Liver Dis 2006;38:854–9.
[22] Iizuka N, Sakaida I, Moribe T, Fujita N, Miura T, Stark M, et al. Elevated levels of circulating cell-free DNA in the blood of patients with hepatitis C virus-associated hepatocellular carcinoma. Anticancer Res 2006;26:4713–9.
[23] Oka H, Saito A, Ito K, Kumada T, Satomura S, Kasugai H. Multicenter prospective analysis of newly diagnosed hepatocellular carcinoma with respect to the percentage of *Lens culinaris* agglutinin-reactive alpha-fetoprotein. J Gastroenterol Hepatol 2001;16:1378–83.
[24] Kasahara A, Hayashi N, Fusamoto H, Kawada Y, Imai Y, Yamamoto H, et al. Clinical evaluation of plasma des-gamma-carboxy prothrombin as a marker protein of hepatocellular carcinoma in patients with tumors of various sizes. Dig Dis Sci 1993;38:2170–6.
[25] Marrero JA, Feng Z, Wang Y, Nguyen MH, Befeler AS, Roberts LR, et al. Alpha-fetoprotein, des-gamma carboxyprothrombin, and lectin-bound alpha-fetoprotein in early hepatocellular carcinoma. Gastroenterology 2009;137:110–8.
[26] Trevisani F, D'Intino PE, Morselli-Labate AM, Mazzella G, Accogli E, Caraceni P, et al. Serum alpha-fetoprotein for diagnosis of hepatocellular carcinoma in patients with chronic liver disease: influence of HBsAg and anti-HCV status. J Hepatol 2001;34:570–5.
[27] Mita Y, Aoyagi Y, Yanagi M, Suda T, Suzuki Y, Asakura H. The usefulness of determining des-gamma-carboxy prothrombin by sensitive enzyme immunoassay in the early diagnosis of patients with hepatocellular carcinoma. Cancer 1998;82:1643–8.
[28] Debruyne EN, Joris R, Delanghe JR. Diagnosing and monitoring hepatocellular carcinoma with alpha-fetoprotein: new aspects and applications. Clin Chim Acta 2008;395:19–26.
[29] Ntzani EE, Ioannidis JP. Predictive ability of DNA microarrays for cancer outcomes and correlates: an empirical assessment. Lancet 2003;362:1439–44.
[30] Brock MV, Hooker CM, Ota-Machida E, Han Y, Guo M, Ames S, et al. DNA methylation markers and early recurrence in stage I lung cancer. N Engl J Med 2008;358:1118–28.
[31] Müller HM, Oberwalder M, Fiegl H, Morandell M, Goebel G, Zitt M, et al. Methylation changes in faecal DNA: a marker for colorectal cancer screening? Lancet 2004;363:1283–5.
[32] Hoque MO, Topaloglu O, Begum S, Henrique R, Rosenbaum E, Van Criekinge W, et al. Quantitative methylation-specific polymerase chain reaction gene patterns in urine sediment distinguish prostate cancer patients from control subjects. J Clin Oncol 2005;23:6569–75.
[33] Chan KC, Lai PB, Mok TS, Chan HL, Ding C, Yeung SW, et al. Quantitative analysis of circulating methylated DNA as a biomarker for hepatocellular carcinoma. Clin Chem 2008;54:1528–36.
[34] Morris MR, Gentle D, Abdulrahman M, Maina EN, Gupta K, Banks RE, et al. Tumor suppressor activity and epigenetic inactivation of hepatocyte growth factor activator inhibitor type 2/SPINT2 in papillary and clear cell renal cell carcinoma. Cancer Res 2005;65:4598–606.
[35] Ntais C, Polycarpou A, Ioannidis JP. SRD5A2 gene polymorphisms and the risk of prostate cancer: a meta-analysis. Cancer Epidemiol Biomark Prev 2003;12: 618–24.
[36] Iizuka N, Hamamoto Y, Oka M. Prediction of cancer outcome with microarrays. Lancet 2005;365:1683–4.

GASTROENTEROLOGY 2010;138:1525–1535

BASIC—LIVER, PANCREAS, AND BILIARY TRACT

Characterization and Functional Analyses of Hepatic Mesothelial Cells in Mouse Liver Development

IZUMI ONITSUKA,* MINORU TANAKA,*,‡ AND ATSUSHI MIYAJIMA*

*Laboratory of Cell Growth and Differentiation and ‡Promotion of Independence for Young Investigators, Institute of Molecular and Cellular Biosciences, University of Tokyo, Tokyo, Japan

BACKGROUND & AIMS: At the onset of liver development, cardiac mesoderm, septum transversum mesenchyme, and endothelial cells are involved in the specification and/or proliferation of hepatoblasts. After this initial stage, however, it is unclear which cells support the proliferation and differentiation of hepatocytes. Here we characterized the nature of mouse hepatic mesothelial cells (MCs) and investigated their role in organogenesis. **METHODS:** Using anti–podocalyxin-like protein 1 (PCLP1) and anti-mesothelin antibodies, we characterized MCs during liver development by immunohistochemistry, flow cytometry, and gene expression analysis. The possible role of MCs in hepatogenesis was investigated by in vitro culture and analysis of Wilms' tumor 1 homologue (WT1) knockout mice. **RESULTS:** PCLP1 was highly expressed in immature MCs, covering the surface of lobes. PCLP1 expression in MCs was down-regulated along with development, whereas mesothelin expression was up-regulated, indicating that these molecules distinguished developmental stages of MCs. The proliferation potential of MCs was high in the fetus and declined after birth. Fetal MCs expressed various growth factors and strongly enhanced the expansion of fetal hepatocytes in vitro, whereas differentiated MCs exhibited less growth factor expression, and differentiated MCs failed to enhance hepatocyte proliferation in vitro. In WT1-deficient embryos, hepatocyte proliferation was impaired due to defective MCs. **CONCLUSIONS: The mesothelium is not only an inert protective sheet covering the parenchyma but also changes its characteristics dynamically during development and plays an active role in organogenesis by promoting expansion of parenchymal cells.**

Keywords: Mesothelium; Mesothelin; Podocalyxin-Like Protein 1; Cell Sorting.

In mouse liver development, hepatic cells are induced from the embryonic endoderm by embryonic day (E) 8.5. The cardiac mesoderm and septum transversum mesenchyme (STM) adjacent to the foregut endoderm produce fibroblast growth factors and bone morphogenetic protein, respectively, to induce liver specification.[1,2] Thereafter, the specified endodermal cells, hepatoblasts, outgrow into the STM to form hepatic cords by the support of endothelial cells (ECs).[3] However, the mechanism of liver development after the liver bud formation remains largely unknown. Although various cytokines have been shown to stimulate proliferation of hepatocytes in vitro (eg, epidermal growth factor, hepatocyte growth factor [HGF], and pleiotrophin [Ptn]),[4,5] it remains elusive how hepatocyte proliferation is supported by surrounding cells in vivo. The lack of tools to precisely identify and isolate different types of liver cells has hampered such investigation. Suksaweang et al have shown that proliferation of hepatocytes is limited to the peripheral region of the hepatic lobe during liver development in the chick.[6] They also suggested that mesenchymal cells located at the periphery of the lobe might provide the microenvironment for hepatocytes to proliferate.[6] However, it was unclear which peripheral mesenchymal cells contribute to hepatogenesis during liver development.

In vertebrates, the periphery of all coelomic organs is covered by a single layer of mesothelial tissue, which provides nonadhesive and protective surfaces. The mesothelium is derived from the lateral plate mesoderm and is believed to play an important role in maintaining normal serosal integrity and functions, such as transport

Abbreviations used in this paper: Ab, antibody; bFGF, basic fibroblast growth factor; Dlk1, delta-like 1 homologue; E, embryonic day; EC, endothelial cell; HGF, hepatocyte growth factor; IHC, immunohistochemistry; MC, mesothelial cell; Mdk, midkine; Msln, mesothelin; OSM, oncostatin M; PCLP1, podocalyxin-like protein 1; PCR, polymerase chain reaction; PD, postnatal day; Ptn, pleiotrophin; RALDH2, retinaldehyde dehydrogenase; RT, reverse-transcription; STM, septum transversum mesenchyme; WT1, Wilms' tumor 1 homologue.

0016-5085/10/$36.00
doi:10.1053/j.gastro.2009.12.059

of fluid and cells in serosal cavities, antigen presentation, inflammation, and tissue repair.[7] During vertebrate development, recent studies have shown that splanchnic mesothelial cells (MCs) delaminate into the parenchymal region and give rise to the vascular cells and mesenchymal cells in multiple coelomic organs, including murine heart,[8] lung,[9] gut,[10] and avian liver.[11] These observations suggest that splanchnic MCs might play important roles in organogenesis as a source of vascular and/or mesenchymal cells in multiple organs. Despite these accumulating reports, however, the precise characteristics of MCs and their roles for the development of parenchymal cells remain largely unknown.

In this study, we show that podocalyxin-like protein 1 (PCLP1) and mesothelin (Msln) are excellent markers to identify and isolate hepatic MCs. PCLP1 is a member of the sialomucin family and was originally identified as a protein highly expressed on glomerular podocytes in avian and mammalian kidneys.[12] It was also reported that PCLP1 is expressed on ECs,[13] immature mesodermal cells such as hemangioblasts, the common progenitor for hematopoietic and vascular endothelial cells,[14] and hematopoietic stem cells.[15] Msln is a glycosylphosphatidylinositol-linked glycoprotein highly expressed in a variety of normal mesothelial tissues, mesotheliomas, and ovarian cancers.[16] Using these cell surface markers, we characterize MCs and show that fetal hepatic MCs are a rich source of multiple growth factors for hepatocytes from early to late stages in liver development, indicating that MC layers play an active role in organogenesis.

BASIC-LIVER, PANCREAS, AND BILIARY TRACT

Materials and Methods

Mice

C57BL/6 mice were purchased from Nihon SLC (Hamamatsu, Japan). Mice were maintained and mated in the institutional animal facility according to the guidelines of the University of Tokyo. The time at midday (12:00) was taken to be E0.5 for plugged mice. WT1 knockout mice[17] were kindly provided by Dr R. Nishinakamura. Embryos were genotyped by polymerase chain reaction (PCR).

Cell Preparation for Flow Cytometric Analysis and Sorting

Livers isolated from embryos were dissociated into a single-cell suspension and stained by antibodies according to the previous report.[18] Cells were analyzed by FACSCalibur (BD Biosciences) or EPICS ALTRA (Beckman Coulter, San Diego, CA). For cell sorting, EPICS ALTRA or autoMACS (Miltenyi Biotec K.K., Tokyo, Japan) instruments were used. Purity of the sorted cell populations estimated by flow cytometry was higher than 90%.

Expansion of Fetal Hepatic MCs and Coculture With Hepatoblasts

Flk1$^-$PCLP1^{high} cells were sorted from E12.5 livers by a cell sorter and expanded in vitro on type IV collagen-coated dishes in α-minimum essential medium containing 10% fetal bovine serum and 50 nmol/L mercaptoethanol, 10 ng/mL oncostatin M (OSM), and 10 ng/mL basic fibroblast growth factor (bFGF). For passage, cells were trypsinized with 0.05% trypsin and 0.5 mmol/L EDTA (Sigma-Aldrich, St. Louis, MO) in phosphate-buffered saline at 37°C for 8 minutes and replated. Delta-like 1 homologue (Dlk1$^+$) fetal hepatoblasts were purified from E14.5 livers using autoMACS as reported previously. A total of 2×10^3 Dlk1$^+$ cells were inoculated into each well of a gelatin-coated 24-well plate with α-minimum essential medium containing 10% fetal bovine serum with or without 1×10^5 in vitro expanded fetal hepatic MCs, which were separated in a 3.0-μm pored Transwell (Corning, NY). As a positive control for proliferation, 25 ng/mL pleiotrophin (Ptn) or 50 ng/mL midkine (Mdk) was added to the culture. After 3 days of culture, cells were stained with Giemsa solution to visualize the colonies or subjected to WST-1 assay (Roche, Diagnostics KK, Tokyo, Japan) according to the manufacturer's protocol. Averages in triplicate cultures were used to determine cell proliferation.

Results

PCLP1 Is Highly Expressed on the Surface Layers of Multiple Coelomic Organs During Embryogenesis

It was reported previously that PCLP1 is widely expressed by "boundary elements," including vasculature, mesothelial linings, and the luminal surface of newly formed cavities in murine embryos.[15] Immunohistochemistry (IHC) of embryonic sections with anti-PCLP1 antibody (Ab) showed that PCLP1 was expressed highly on the surface of multiple coelomic organs such as heart, lung, liver, and stomach (data not shown). Because all the coelomic organs are covered by a single layer of MCs, cells with an intense PCLP1 signal were suggested to be the mesothelial lining.

On E9.5 tissue sections, double staining with anti-PCLP1 Ab and anti-Dlk1 Ab, which recognizes fetal hepatoblasts,[18,19] showed the presence of PCLP1$^+$ cells in the STM, where hepatic cords form with Dlk1$^+$ hepatoblasts emerging from the foregut endoderm (Figure 1*A*). At E10.5, a monolayer of cells with an intense PCLP1 signal was detected on the surfaces of dorsal lobes, and these cells covered each hepatic lobe completely at E12.5 (Figure 1*A*). While the signals were continuously detected at E16.5, their frequency and intensity were reduced at postnatal day (PD) 4, and no PCLP1 signal was detected on the surface of adult livers (Figure 1*A*). These results suggested that the PCLP1 expression on the surface of hepatic lobes is regulated in a stage-specific manner. By

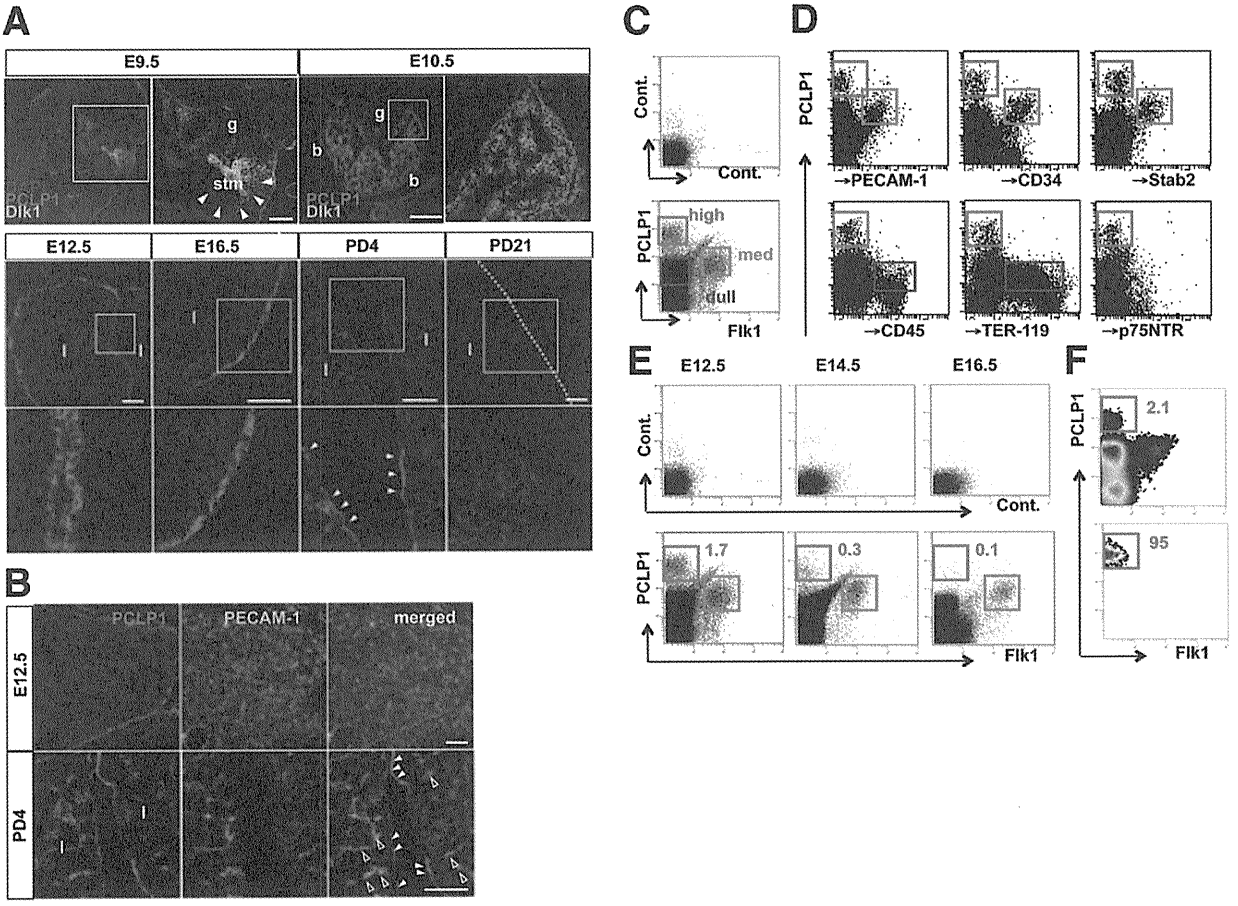

Figure 1. IHC and flow cytometry with anti-PCLP1 Ab in the developing liver. (*A* and *B*) IHC with anti-PCLP1 (*red*), anti-Dlk1 (*green* in *A*), and anti–PECAM-1 (*green* in *B*) Abs and 4′,6-diamidino-2-phenylindole (*blue* in *A*). Higher-magnification images of the *boxed regions* in *A* are shown to the right (E9.5 and E10.5) or underneath (E12.5 to PD21). The *dotted line* in *A* (PD21) delineates the periphery of the hepatic lobe. *Arrowheads* indicate PCLP1^{+} cells in the STM region (E9.5) or in the mesothelial layer (PD4 in *A* and *B*), respectively. *Open arrowheads* in *B* indicate PECAM1^{+}PCLP1^{med} sinusoidal ECs. g, gut; stm, septum transversum mesenchyme; b, body wall; l, lobe. *Scale bars* = 100 μm. (*C*) Flow cytometry of E12.5 liver cells using anti-PCLP1 and anti-Flk1 Abs. *Red*, *green*, and *blue lines* in the *lower panel* indicate Flk1^{-}PCLP1^{high}, Flk1^{+}PCLP1^{med}, and Flk1^{-}PCLP1^{dull} cell populations, respectively. (*D*) Flow cytometry of E12.5 liver cells using anti-PCLP1 Ab and other cell surface molecules. *Red*, *green*, and *blue lines* in each *panel* indicate PCLP1^{high}, PCLP1^{med}, and PCLP1^{dull} cell populations, respectively. (*E*) Flow cytometry of E12.5, E14.5, and E16.5 liver cells using anti-PCLP1 and anti-Flk1 Abs. *Red* and *green lines* in each *lower panel* indicate Flk1^{-}PCLP1^{high} and Flk1^{+}PCLP1^{med} cells, respectively. The number indicates the percentage of Flk1^{-}PCLP1^{high} cells. (*F*) Flow cytometry of E12.5 liver cells before (*upper panel*) and after (*lower panel*) sorting of Flk1^{-}PLCP1^{high} cells by a cell sorter. Sorting gates are indicated by *red lines*. Numbers in each *panel* indicate the percentage of Flk1^{-}PCLP1^{high} cells.

contrast, weak PCLP1 signals were observed in the parenchymal region from E12.5 to adults. In accordance with the previous report that PCLP1 is expressed on ECs,[13] weak PCLP1 signals colocalized with PECAM-1, an endothelial marker, in the parenchymal region; however, no colocalization occurred with strong PCLP1 signals in the mesothelial lining (Figure 1*B*).

Flow Cytometric Analysis of PCLP1^{+} Cells in Fetal Liver

Flow cytometry of E12.5 fetal liver cells with anti-PCLP1 Ab and anti-Flk1 Ab, which detects ECs, revealed that PCLP1^{+} cells could be fractionated into at least 3 populations, PCLP1^{high}, PCLP1^{med}, and PCLP1^{dull} cells, based on the expression levels of PCLP1 (Figure 1*C*). Multicolor flow cytometry revealed that PCLP1^{med} cells were positive for several EC markers but not for CD45 (Figure 1*D* and data not shown). PCLP1^{dull} cells contained TER-119^{+} erythroids and CD45^{+} leukocytes (Figure 1*D*), consistent with the previous report.[15] By contrast, PCLP1^{high} cells were completely negative for EC and blood cell markers as well as the hepatic stellate cell marker p75 neurotrophin receptor[20] (Figure 1*C*–*E*), indicating that the Flk1^{-}PCLP1^{high} cell population was distinct from these nonparenchymal cells. The fraction of Flk1^{-}PCLP1^{high} cells in total fetal liver cells decreased as development progressed (Figure 1*E*).

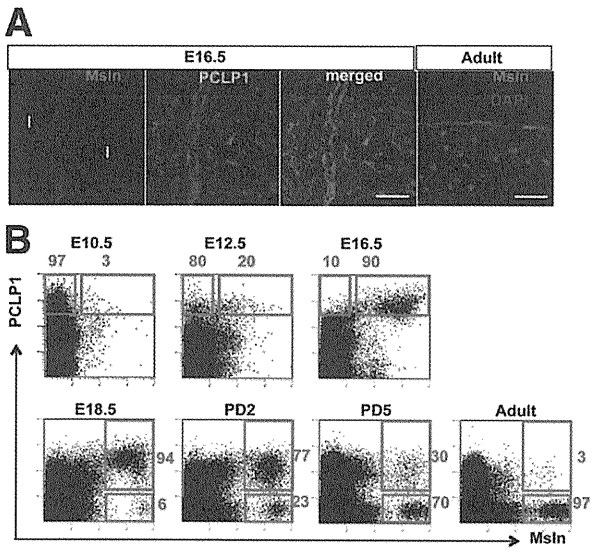

Figure 2. Expression of PCLP1 and Msln in the mesothelial layer during liver development. (*A*) IHC of liver sections with anti-Msln (*red*) and anti-PCLP1 (*green*) Abs. l, lobe. *Scale bars* = 80 μm. (*B*) Flow cytometry of liver cells with anti-PCLP1 and anti-Msln Abs. *Red lines* in each panel indicate PCLP1^{high} (*upper panels*) and Msln^{+} (*lower panels*) cell populations, respectively. The cells of whole livers (E10.5 and E12.5) and surgically separated mesothelial tissues (E16.5, E18.5, PD2, PD5, and Adult) were used for flow cytometry. Numbers in each *panel* indicate the percentage of each cell population in PCLP1^{high} (*upper panels*) or in Msln^{+} (*lower panels*) cells.

Flow cytometry of surgically separated E16.5 livers into mesothelial and nonmesothelial tissues under a stereomicroscope revealed that Flk1^{-}PCLP1^{high} cells were present exclusively in the mesothelial tissue, while Flk1^{+}PCLP1^{med} cells were detected mainly in the nonmesothelial tissue (Supplementary Figure 1*A* and *B*). These results indicated that the PCLP1^{high} and PCLP1^{med} cells by flow cytometry correspond to fetal MCs and ECs detected by IHC, respectively, and that PCLP1^{high} cells could be isolated by a cell sorter with high purity (Figure 1*F*).

Expression of PCLP1 and Msln in Hepatic MCs During Liver Development

Msln is known to be a general marker for MCs. IHC showed that a single cell layer of mesothelial lining was specifically stained by both anti-Msln and anti-PCLP1 Abs in E16.5 liver sections (Figure 2*A*). In contrast to the lack of PCLP1 expression in adult MCs (Figure 1*A*), Msln was strongly expressed on adult MCs (Figure 2*A*) but not on fetal livers at earlier stages (data not shown). Cells highly expressing Msln were exclusively detected by flow cytometry in the surgically separated mesothelial tissue in PD0 and adult livers (Supplementary Figure 1*C*). These results suggested that MCs changed surface phenotypes from PCLP1^{+} to Msln^{+} during development. Consistent with the results of IHC, flow cytometry clearly showed that most of the PCLP1^{high} cells were Msln^{-} in E10.5 liver cell suspensions (Figure 2*B*). Interestingly, the fraction of Msln^{+} cells in the PCLP1^{high} cell population increased as fetal development progressed, while PCLP1^{+} cells in the Msln^{+} population decreased gradually after birth (Figure 2*B*). These results indicated that the expression of PCLP1 and Msln is developmentally regulated, and 3 developmental stages of MCs can be distinguished based on the expression of these 2 markers, that is, PCLP1^{high}Msln^{-}, PCLP1^{+}Msln^{+}, and PCLP1^{-}Msln^{+} MCs are the immature, intermediate, and mature stages of MCs, respectively.

Development of an In Vitro Culture System for Fetal MCs

To further characterize fetal MCs, we have developed an in vitro culture system for fetal MCs isolated by a cell sorter based on the expression of PCLP1 and/or Msln. The proliferation potential of MCs was determined by in vitro colony formation assay (see Supplementary Materials and Methods). Total numbers of colonies formed from 1 × 10^3 MCs isolated from E12.5, E18.5, and PD7 livers were 251.0 ± 5.7, 229.7 ± 19.7, and 95.3 ± 7.1, respectively, indicating that fetal hepatic MCs possessed higher proliferation potential than postnatal MCs. Adult hepatic MCs formed very few colonies (~3/1000 MCs; Figure 3*A* and *B*). Only PCLP1^{+}Msln^{+} MCs formed large colonies consisting of more than 300 cells, whereas the size of colonies formed from PD7 MCs was small (Figure 3*A* and *B*), indicating that hepatic MCs at the intermediate stage proliferate most actively and the proliferation potential of hepatic MCs declines after birth.

Interestingly, the cultivation of E12.5 PCLP1^{high}Msln^{-} cells changed the expression of PCLP1 and Msln, similar to the developmental change in vivo as shown in Figure 2*B* (Figure 3*C*). In this culture condition without exogenous cytokines, fetal MCs proliferated modestly but their proliferation ceased within several days. Additionally, they became PCLP1^{-}Msln^{+} MCs, a phenotype similar to adult MCs (Figure 3*C* and *D*). We found that addition of OSM and bFGF to culture medium synergistically promoted the expansion of fetal MCs (Figure 3*D*). Furthermore, 49% of the E12.5 PCLP1^{high} MCs maintained expression of PCLP1 after 6 days of cultivation in the presence of OSM and bFGF, while only 8% of the cells did so in their absence (Figure 3*E*). The continuous presence of OSM and bFGF in the culture medium maintained the expression of PCLP1 after the first passage, while their removal resulted in rapid down-regulation of PCLP1 expression and up-regulation of Msln expression (Figure 3*F* and Supplementary Figure 2). These results strongly suggested that OSM and bFGF could maintain immature characteristics of fetal MCs, whereas MCs proceeded to differentiate without them.

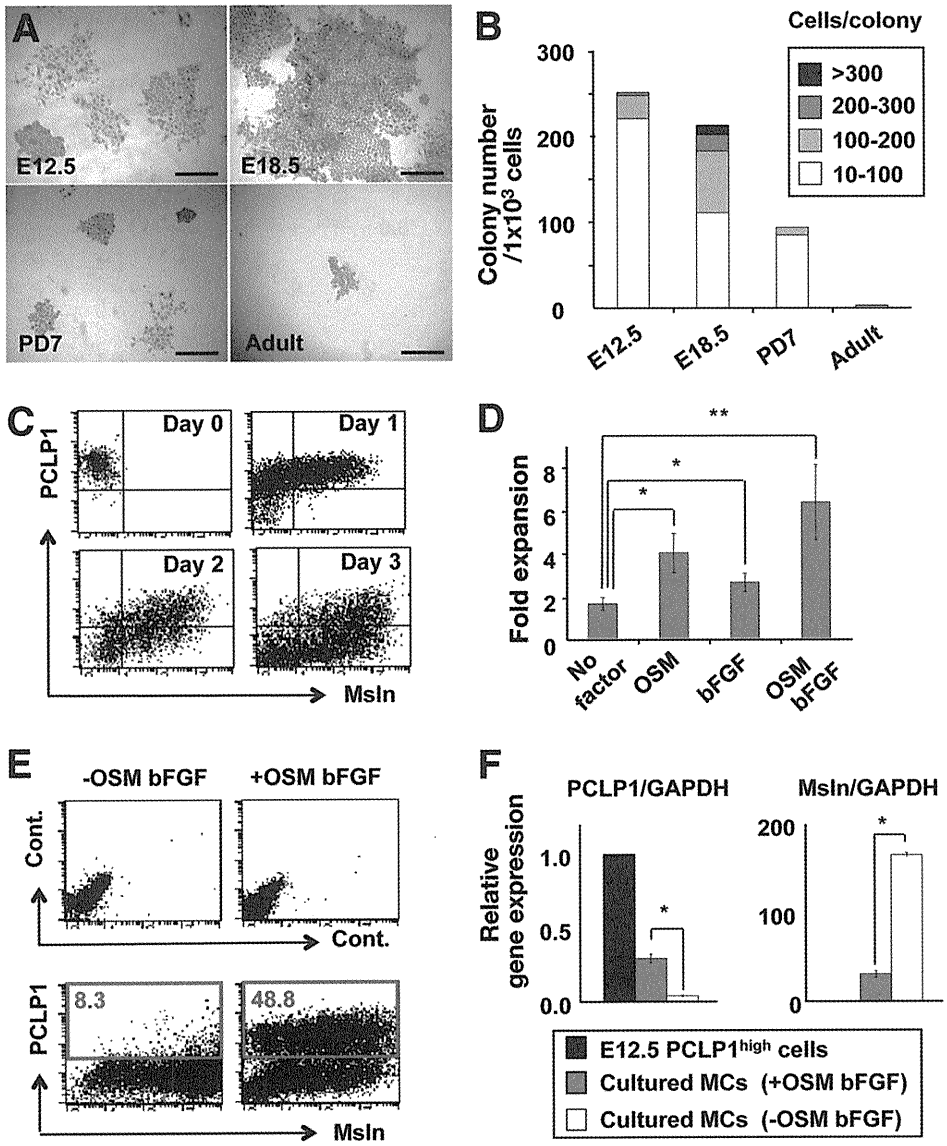

Figure 3. Expansion and differentiation of fetal MCs in vitro. (*A*) Colony-forming activity of hepatic MCs isolated from various stages of developing liver. Morphology of colonies formed from immature (E12.5), intermediate (E18.5), or mature (PD7 and Adult) MCs are shown. Colonies were stained with Giemsa solution after 6 days in culture. *Scale bars* = 80 μm. (*B*) Quantification of colony-forming potentials of MCs isolated from E12.5, E18.5, PD7, or adult liver. Averages of 3 wells for each sample are indicated. (*C*) Flow cytometry of cultured PCLP1^{high}Msln^{-} cells. Sorted cells from E12.5 liver were incubated and stained with anti-PCLP1 and anti-Msln Abs at the indicated time points. (*D*) Proliferation of fetal MCs in vitro. Flk1^{-}PCLP1^{high} cells sorted from E12.5 livers were cultured in the presence or absence of cytokines (10 ng/mL each) as indicated, and cell numbers were determined at day 6. Averages of 3 wells for each sample are shown. $^{*}P < .05$, $^{**}P < .01$; Student *t* test. (*E*) Flow cytometry of cultured MCs with anti-PCLP1 and anti-Msln Abs. Freshly isolated E12.5 Flk1^{-}PCLP1^{high} cells were cultured for 6 days in the presence or absence of OSM and bFGF and analyzed by flow cytometry. *Red lines* and *numbers* in the *lower panels* indicate PCLP1^{+} cell populations and their percentages, respectively. (*F*) Quantitative RT-PCR analysis for expression of PCLP1 and Msln in freshly isolated E12.5 PCLP1^{high} cells and cultured MCs. The actual ratios of marker/GAPDH in PLCP1^{high} cells and cultured cells (+OSM bFGF or −OSM bFGF) are as follows: PCLP1, 2.1×10^{-1}, 8.0×10^{-2}, and 7.5×10^{-3}; Msln, 1.8×10^{-3}, 6.6×10^{-2}, and 3.0×10^{-1}. $^{*}P < .00003$; Student *t* test.

Fetal Hepatic MCs Are a Rich Source of Growth Factors for Hepatoblasts

It is known that MCs possess characteristics of both epithelial and mesenchymal cells,[7] but precise information about gene expression and other developmental characteristics of MCs remains limited. Therefore, microarray analysis was performed to compare gene expression profiles of E12.5 PCLP1^{high}Msln^{-} MC progenitors with adult Msln^{+} MCs (National Center for Biotechnology Information Gene Expression Omnibus accession no. GSE 18937). We found that MCs changed their gene expression profile drastically dur-

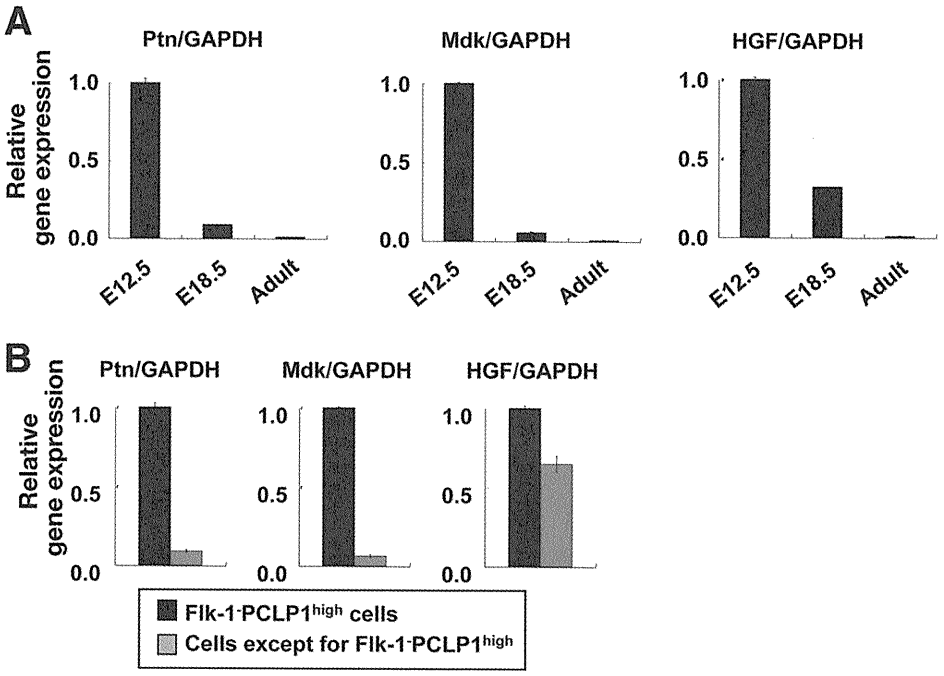

Figure 4. Expression of growth factors in liver cells. (*A*) Quantitative RT-PCR analysis for growth factors in MCs at distinct developmental stages. E12.5 Flk1^{-}PCLP1^{high} cells, E18.5 Msln^{+} cells, and adult Msln^{+} cells were isolated by a cell sorter and used for analyses. The actual ratios of factor/GAPDH in E12.5, E18.5, and adult MCs are as follows: Ptn, 3.9×10^{-1}, 4.0×10^{-2}, and 2.9×10^{-3}; Mdk, 1.0×10^{-1}, 6.1×10^{-3}, and 5.1×10^{-4}; HGF, 2.6×10^{-3}, 1.1×10^{-3}, and 4.7×10^{-4}. (*B*) Quantitative RT-PCR analysis of growth factors in Flk1^{-}PCLP1^{high} cells and the other cells at E12.5. The actual ratios of growth factor/GAPDH in Flk1^{-}PCLP1^{high} cells and the other cells are as follows: Ptn, 3.9×10^{-1} and 4.1×10^{-2}; Mdk, 1.0×10^{-1} and 7.8×10^{-3}; HGF, 2.6×10^{-3} and 1.6×10^{-3}.

ing development and that various signaling molecules were expressed in both fetal and adult MCs. In the list of soluble mediators whose expression in E12.5 MCs was more than 5-fold higher than in adult MCs (Supplementary Table 1), there were several growth factors known to promote proliferation of hepatocytes. Ptn is known to be a mitogen for adult hepatocytes[4,5] and was shown to be expressed highly in the STM and the hepatic MC layer of rat embryos.[5] Mdk is a molecule structurally related to Ptn.[4] Consistent with the microarray analysis, quantitative reverse-transcription (RT)-PCR analysis revealed that Ptn and Mdk were highly expressed in E12.5 MCs and became gradually down-regulated during ontogeny (Figure 4*A*). HGF was also expressed in E12.5 MCs, although its expression level was much lower than those of Ptn and Mdk (see the legend for Figure 4*A*). Furthermore, these growth factors were expressed more abundantly in MCs at E12.5 compared with non-MCs that contained hepatocytes, ECs, mesenchymal cells, and blood cells (Figure 4*B*). The expression of insulin-like growth factor 2 was detected at high levels in fetal MCs, although it was also expressed in fetal hepatocytes (data not shown). Importantly, all of these factors were remarkably down-regulated during development and were hardly detectable in adult MCs (Figure 4*A*). These observations suggested the intriguing possibility that fetal hepatic MCs play an active role in the proliferation and/or differentiation of hepatic cells in the developing liver.

Fetal MCs Promote Expansion of Hepatoblasts in a Paracrine Manner by Secreting Soluble Factors

To examine whether fetal MCs contribute to proliferation of hepatoblasts, we designed a coculture system of fetal hepatocytes with fetal MCs. Because the number of MCs isolated from fetal livers was too small for such experiments, we took advantage of fetal MCs expanded in vitro. Fetal hepatoblasts were isolated from E14.5 livers with anti-Dlk1 Ab as reported previously[18] and cultured with or without fetal MCs expanded in vitro using a 3-μm pored Transwell (Figure 5*A*). Hepatoblasts proliferated actively in the presence of Ptn or Mdk (Figure 5*B*) and in the coculture with MCs (Figure 5*C* and *D*), which was confirmed by WST-1 assay. MCs isolated from a later stage (E18.5) also enhanced the proliferation of fetal hepatocytes, and E16.5 hepatocytes also proliferated by coculture with later-stage MCs (Supplementary Figure 3 and data not shown). Importantly, MCs cultured without OSM and bFGF before coculture failed to stimulate the proliferation of hepatoblasts (Figure 5*C*). These MCs also exhibited a cell surface phenotype similar to differentiated MCs (Figure 3*E* and *F*), and growth factor expression was remarkably reduced, similar to adult MCs (Figures 5*E* and 4*A*). By contrast, MCs cultured in the presence of OSM and bFGF expressed growth factors at levels comparable to E18.5 MCs (Figures 5*E* and 4*A*). These results indicated that fetal hepatic MCs possess the potential to promote the proliferation of hepatocytes by secreting soluble factors, and the 2 types of MCs used for coculture exhibit the characteristics of fetal undifferentiated MCs and adult MCs in vivo, respectively.

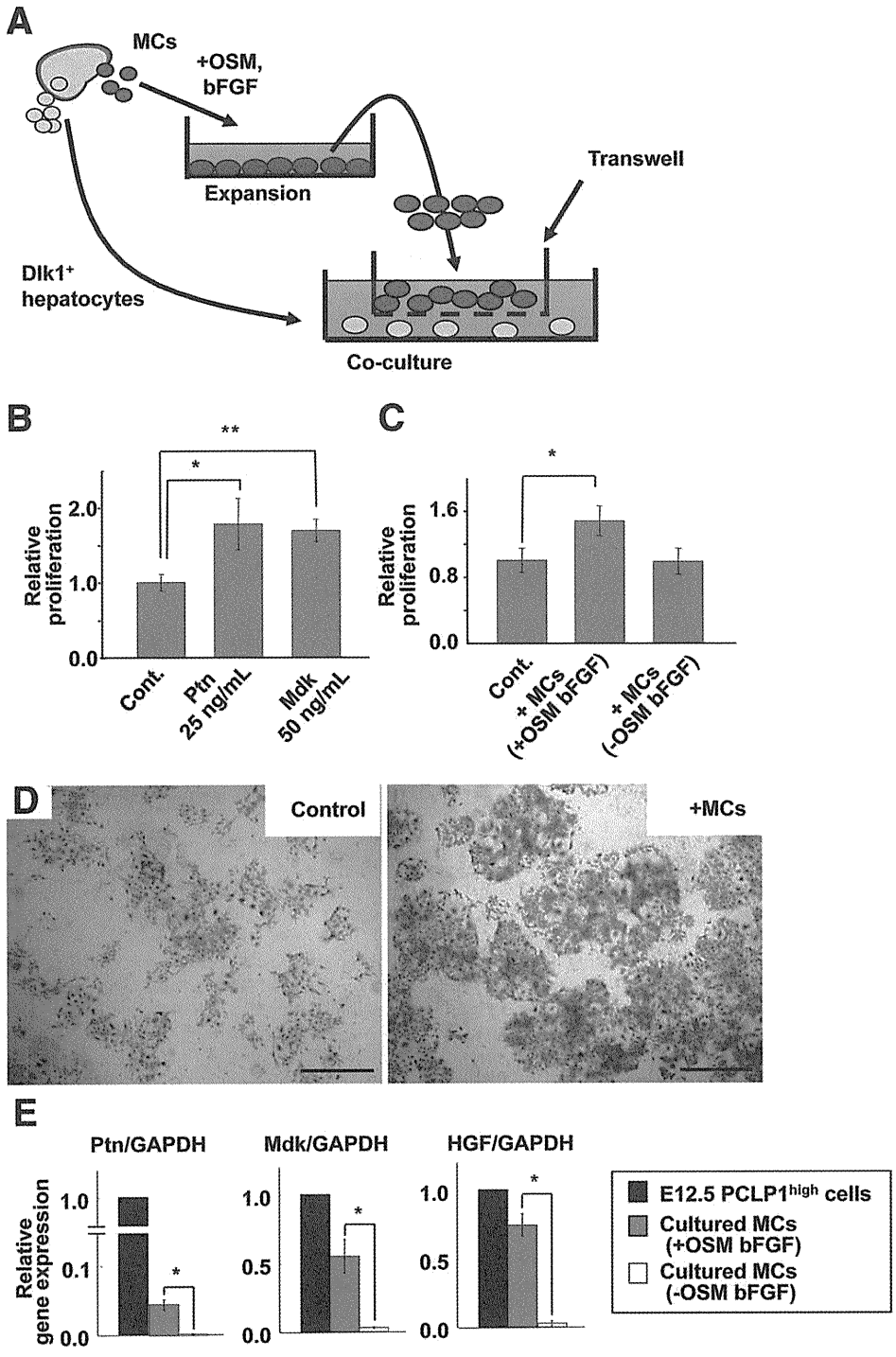

Figure 5. Hepatic MCs promote the proliferation of hepatoblasts in the coculture system. (*A*) The coculture system of fetal hepatoblasts and hepatic MCs separated by Transwell. After culturing of freshly isolated MCs in the presence of OSM and bFGF, the expanded MCs were used for coculture with Dlk1$^+$ hepatoblasts. (*B*) Proliferation of hepatoblasts in coculture system. Dlk1$^+$ cells sorted from E14.5 livers were cultured in the presence of growth factors as indicated. Growth of hepatocytes was measured by WST-1 assay after 4 days of culture. The averages for 3 wells of each sample are shown. $^*P < .03$; $^{**}P < .004$; Student *t* test. (*C*) Proliferation of E14.5 Dlk1$^+$ cells cultured with in vitro expanded E12.5 MCs. After primary expansion of MCs, the cells were cultured for an additional 5 days in the presence or absence of OSM and bFGF before coculture. Growth of hepatocytes was measured by WST-1 assay as in *B*. $^*P < .007$; Student *t* test. (*D*) Appearance of hepatocytes stained with Giemsa solution after 3 days of coculture. (*E*) Quantitative RT-PCR analysis of growth factors in freshly isolated E12.5 PCLP1^{high} cells and cultured MCs. The actual ratios of marker/GAPDH in PLCP1^{high} cells and cultured cells with OSM and bFGF (+OSM bFGF) or without them (−OSM bFGF) before coculture are as follows: Ptn, 1.4, 5.7 × 10^{-2}, and 2.6 × 10^{-3}; Mdk, 1.8 × 10^{-2}, 1.0 × 10^{-2}, and 5.5 × 10^{-4}; HGF, 4.1 × 10^{-4}, 3.0 × 10^{-4}, and 1.1 × 10^{-5}. $^*P < .0005$; Student *t* test.

In Vivo Function of Fetal Hepatic MCs

Wilms' tumor 1 homologue (WT1) is a Zn finger protein that is known to play a critical role in organogenesis of multiple organs, including the kidney, heart, diaphragm, spleen, gonad, and liver. WT1 is also known as a marker for the mesothelial lineage,[7] and it is believed to be a regulator of mesothelial development. In mouse fetal liver, WT1 was reported to be expressed strongly in coelomic epithelial cells,[21] which correspond to hepatic MCs. In fact, WT1 was mainly expressed in MCs, whereas its expression was hardly detectable in non-MCs, including hepatocytes, ECs, mesenchymal cells, and blood cells

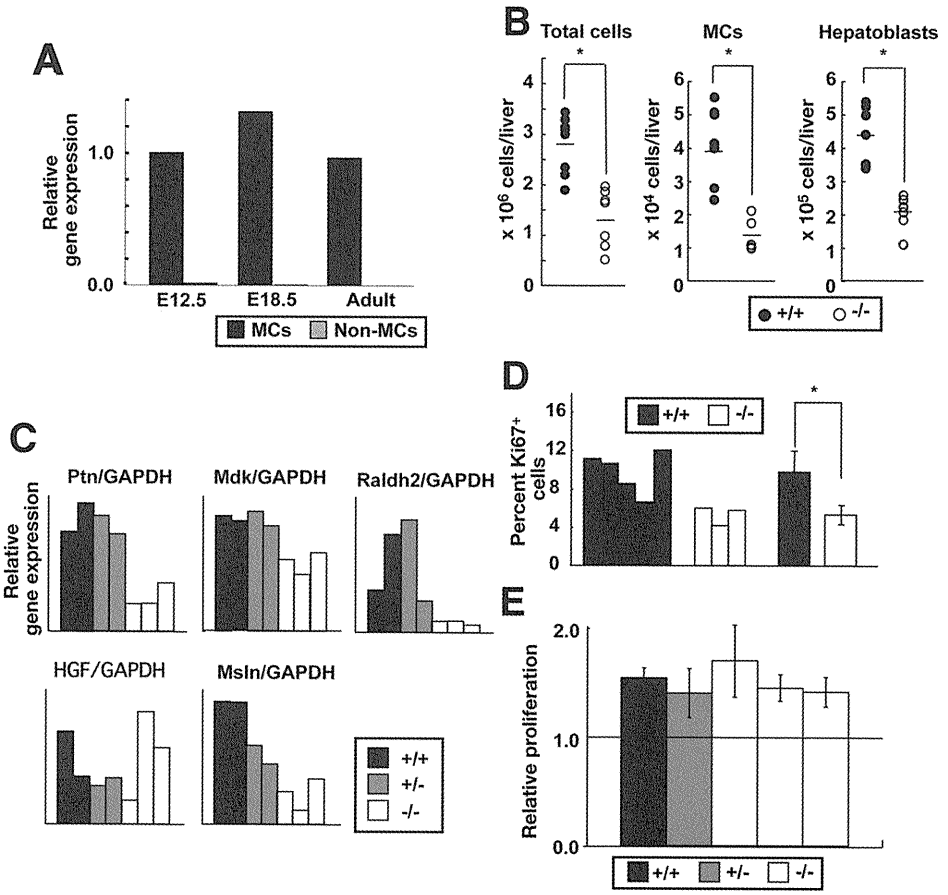

Figure 6. Characteristics of hepatic MCs in WT1-deficient embryos. (*A*) Quantitative RT-PCR analysis of WT1 expression in MCs or non-MCs. The relative gene expression of WT1/GAPDH in MCs and non-MCs at distinct developmental stages is shown. The actual ratios of WT1/GAPDH in MCs and non-MCs for E12.5, E18.5, and adults are 2.4×10^{-4} and 3.2×10^{-6}, 3.7×10^{-4} and 3.5×10^{-7}, and 2.3×10^{-4} and 2.8×10^{-6}, respectively. (*B*) The numbers of total fetal liver cells (*left panel*; +/+, n = 8; −/−, n = 8), PCLP1^{high} cells (*middle panel*; +/+, n = 7; −/−, n = 6), and Dlk1^{+} cells (right panel, +/+, n = 7; −/−, n = 6) per liver of E13.5 embryos are shown. *$P < .0007$; Student *t* test. (*C*) Quantitative RT-PCR analysis in PCLP1^{high} MCs of E13.5 littermates. Relative gene expression is shown. *Filled*, *gray*, and *open bars* indicate an individual embryo with +/+, +/−, and −/− genotype, respectively. (*D*) The ratio of Ki67^{+} cells in PCLP1^{high} MCs between E13.5 WT1$^{+/+}$ and WT1$^{-/-}$ livers of littermates. The *right bars* show the difference between the 2 genotypes. *$P < .02$; Student *t* test. (*E*) Proliferation potential of Dlk1^{+} hepatoblasts derived from E13.5 WT1$^{+/+}$, WT1$^{+/-}$, and WT1$^{-/-}$ livers. Dlk1^{+} hepatoblasts of littermates with each genotype were sorted by a cell sorter and cocultured with or without in vitro expanded E12.5 WT1$^{+/+}$ MCs. Growth of hepatocytes was measured by WST-1 assay in triplicate cultures after 4 days of coculture. The ratios of the WST-1 value in culture with MCs to that without MCs are shown for each genotype. Note that there is no significant difference among genotypes. The experiment was repeated twice with similar results.

in the developing liver (Figure 6*A*). Consistent with a previous report,[21] WT1$^{-/-}$ embryos had smaller livers with incomplete lobulation compared with littermates with WT1$^{+/+}$ or WT1$^{+/-}$ genotypes at E13.5 (Supplementary Figure 4*A* and data not shown). The percentages of Flk1^{-}PCLP1^{high} MC progenitors in WT1$^{-/-}$ fetal livers were not reduced significantly compared with their littermates by flow cytometry (Supplementary Figure 4*B* and data not shown). However, the numbers of Flk1^{-}PCLP1^{high} MCs, Dlk1^{+} hepatoblasts, and total fetal liver cells were all reduced in WT1$^{-/-}$ animals (Figure 6*B*). Next, we isolated MCs to examine the expression of growth factors by quantitative RT-PCR. Ptn and Mdk were reduced in WT1$^{-/-}$ hepatic MCs compared with the littermates with WT1$^{+/+}$ or WT1$^{+/-}$ genotypes (Figure 6*C*). The expression of Msln in WT1$^{-/-}$ MCs was also severely reduced at E13.5, indicating that MC differentiation may also be impaired in WT1-deficient livers. In addition, the expression of retinaldehyde dehydrogenase 2 (RALDH2) was significantly reduced in WT1$^{-/-}$ MCs, consistent with the notion that retinoic acid regulates proliferation of MCs in vivo.[21] Proliferation of MCs might also be altered in these embryos. The percentages of Ki67^{+} cells in PCLP1^{high} MCs isolated from WT1$^{-/-}$ embryos were significantly reduced compared with those of WT1$^{+/+}$ embryos (Figure 6*D*). Coculture of Dlk1^{+}

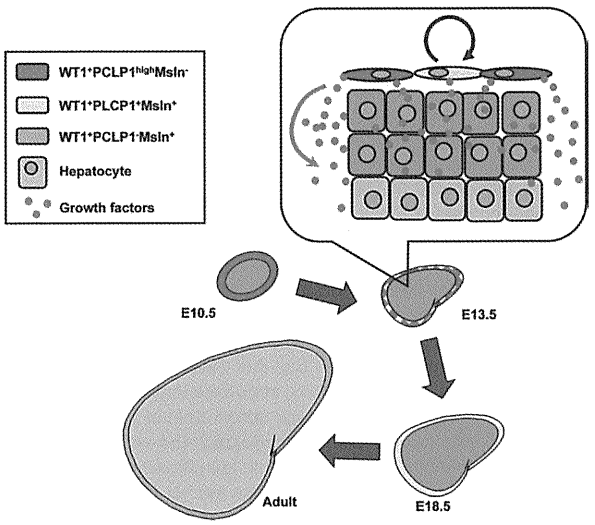

Figure 7. A model for hepatic MC development and its role in liver organogenesis. At an early stage of liver development, PCLP1^{high}Msln^{-} immature MCs cover the hepatic lobes (E10.5–12.5, *red*). The expression of Msln is up-regulated in MCs during fetal liver development, and most of the MCs become PCLP1^{+}Msln^{+} around birth (E18.5, *light yellow*). MCs provide hepatoblasts with multiple growth factors and they also proliferate actively during fetal stages, contributing to liver organogenesis. After birth, MCs become PCLP1^{-}Msln^{+} (*light green*), and their proliferation potential declines. MCs then switch their function from a niche for hepatoblasts to nonadhesive protective surfaces.

hepatocytes from WT1$^{-/-}$ or WT1$^{+/+}$ livers with WT1$^{+/+}$ MCs showed no significant difference in proliferation of hepatocytes among the different genotypes, indicating that the reduced proliferation of hepatocytes in WT1$^{-/-}$ fetal livers was not due to defects in hepatocytes (Figure 6*E*). From these results, we concluded that WT1-null hepatic MCs are defective in proliferation and the production of growth factors. These results strongly suggested that impaired development of hepatic MCs results in decreased proliferation of hepatocytes as well as abnormal morphogenesis of the liver.

Discussion

In this study, we show that splanchnic MCs are not only an inert protective sheet for coelomic organs but also change their characteristics dynamically during organogenesis. In the liver, at least 3 distinct developmental stages of MCs are recognized based on the expression of PCLP1 and Msln (Figure 7). PCLP1^{high}Msln^{-} immature MC progenitors at E10.5 define the border of each hepatic lobe. Furthermore, the proliferation and gene expression profile of hepatic MCs change dramatically during development. In particular, fetal hepatic MCs were shown to express various soluble factors, including hepatocyte mitogens such as Ptn, Mdk, and HGF, indicating that MCs function as a rich source of growth factors for hepatic cells in liver development (Figures 4 and 7). In fact, coculture experiments using MCs and Dlk1^{+} fetal hepatocytes clearly show that MCs provide growth factors for hepatocytes. Considering that mesenchymal cells derived from STM contribute to the commitment of foregut endodermal cells into the hepatic lineage and to the outgrowth of hepatoblasts at the onset of liver development, it is not surprising that the lateral plate mesoderm-derived mesothelial tissue plays an active role in liver development as a producer of growth factors. Consistent with the previous report by Suksaweang et al,[6] we observed that Ki67^{+}HNF4α^{+} proliferating hepatocytes were present more frequently in the peripheral region than in the central region of the lobes in developing mouse liver (Supplementary Figure 5 and Supplementary Table 2). These observations suggest that MCs contribute to liver growth and morphogenesis by providing mitotic stimuli and/or microenvironment for hepatocytes.

This idea is strongly supported by the analysis of WT1-deficient mice. Ijpenberg et al recently reported that the livers of WT1 mutant embryos are small, showing defects in the proliferation of coelomic epithelial cells and hepatocytes, lobulation, and differentiation of stellate cells during liver development.[21] Coelomic epithelial cells lining the liver of WT1-null embryos showed the reduction of Raldh2 expression, suggesting possible involvement of the retinoic acid signaling pathway in liver development as in the case of heart development that requires WT1-expressing epicardial cells and Raldh2.[22,23] However, it had been unclear why proliferation of hepatocytes was also impaired in WT1-deficient fetal livers. Isolation and characterization of PCLP1^{high} MCs from WT1$^{-/-}$ mice in this study show that proliferation of MCs and their production of growth factors, including Ptn and Mdk, are impaired in these embryos, whereas Dlk1^{+} cells from WT1$^{-/-}$ livers proliferate normally in response to WT1$^{+/+}$ MCs. The expression level of HGF was not affected in the absence of WT1, although the expression level of HGF in WT1$^{+/+}$ MCs was much lower than that of Ptn and Mdk. Thus, it is strongly suggested that the growth retardation of WT1-deficient livers is mainly due to the reduced proliferation of hepatic MCs and their insufficient production of mitogens for hepatocytes. Importantly, because MCs express various growth factors, there might be factors other than Ptn, Mdk, and HGF that also stimulate proliferation of hepatocytes.

Previous studies showed that WT1-expressing epicardial and serosal MCs are a source of coronary and gut vasculogenic cells, respectively.[8,10] It is thus of great interest to know whether immature PCLP1^{high}Msln^{-} cells also possess the potential to differentiate into nonmesothelial lineages. In fact, Pérez-Pomares et al reported that liver sinusoidal endothelial cells and mural cells in avian embryos were derived from the mesothelium.[11] We observed that some ALCAM^{+} cells were generated in the culture of E12.5 PCLP1^{high}ALCAM^{-} MCs (Supplemen-

tary Figure 6). Because ALCAM is specifically expressed in submesothelial cells that underlie the hepatic MC layer,[24] MCs may have a potential to give rise to those mesenchymal cells. Further studies on the differentiation potential of MCs may provide new insights in liver organogenesis.

Fetal liver is the major hematopoietic organ and contains numerous blood cells, which also contribute to hepatogenesis. We previously showed that OSM produced from blood cells stimulates the differentiation of fetal hepatoblasts in vitro.[25] After birth, hematopoiesis shifts to the bone marrow and OSM expression decreases in the liver. In this report, we show that OSM stimulates the proliferation of fetal hepatic MCs and maintains their immature characteristics, including the ability to support the proliferation of hepatoblasts. These results suggest the possible link between hematopoiesis and the proliferation of MCs and hepatoblasts in fetal liver and that OSM may play a role for the coordination of these cells.

In conclusion, this study reveals dynamic changes in characteristics of hepatic MCs during development and shows that hepatic MCs play an active role in organogenesis by providing growth factors for parenchymal cells. Besides liver development, fetal MCs may also be actively involved in the development of other organs.

Supplementary Material

Note: To access the supplementary material accompanying this article, visit the online version of *Gastroenterology* at www.gastrojournal.org, and at doi: 10.1053/j.gastro.2009.12.059.

References

1. Jung J, Zheng M, Goldfarb M, et al. Initiation of mammalian liver development from endoderm by fibroblast growth factors. Science 1999;284:1998–2003.
2. Rossi JM, Dunn NR, Hogan BL, et al. Distinct mesodermal signals, including BMPs from the septum transversum mesenchyme, are required in combination for hepatogenesis from the endoderm. Genes Dev 2001;15:1998–2009.
3. Matsumoto K, Yoshitomi H, Rossant J, et al. Liver organogenesis promoted by endothelial cells prior to vascular function. Science 2001;294:559–563.
4. Muramatsu T. Midkine and pleiotrophin: two related proteins involved in development, survival, inflammation and tumorigenesis. J Biochem 2002;132:359–371.
5. Asahina K, Sato H, Yamasaki C, et al. Pleiotrophin/heparin-binding growth-associated molecule as a mitogen of rat hepatocytes and its role in regeneration and development of liver. Am J Pathol 2002;160:2191–2205.
6. Suksaweang S, Lin CM, Jiang TX, et al. Morphogenesis of chicken liver: identification of localized growth zones and the role of beta-catenin/Wnt in size regulation. Dev Biol 2004;266:109–122.
7. Herrick SE, Mutsaers SE. Mesothelial progenitor cells and their potential in tissue engineering. Int J Biochem Cell Biol 2004;36:621–642.
8. Perez-Pomares JM, Carmona R, Gonzalez-Iriarte M, et al. Origin of coronary endothelial cells from epicardial mesothelium in avian embryos. Int J Dev Biol 2002;46:1005–1013.
9. Que J, Wilm B, Hasegawa H, et al. Mesothelium contributes to vascular smooth muscle and mesenchyme during lung development. Proc Natl Acad Sci U S A 2008;105:16626–16630.
10. Wilm B, Ipenberg A, Hastie ND, et al. The serosal mesothelium is a major source of smooth muscle cells of the gut vasculature. Development 2005;132:5317–5328.
11. Pérez-Pomares JM, Carmona R, Gonzalez-Iriarte M, et al. Contribution of mesothelium-derived cells to liver sinusoids in avian embryos. Dev Dyn 2004;229:465–474.
12. Kerjaschki D, Sharkey DJ, Farquhar MG. Identification and characterization of podocalyxin—the major sialoprotein of the renal glomerular erythelial cell. J Cell Biol 1984;98:1591–1596.
13. Horvat R, Hovorka A, Dekan G, et al. Endothelial cell membranes contain podocalyxin—the major sialoprotein of visceral glomerular epithelial cells. J Cell Biol 1986;102:484–491.
14. Hara T, Nakano Y, Tanaka M, et al. Identification of podocalyxin-like protein 1 as a novel cell surface marker for hemangioblasts in the murine aorta-gonad-mesonephros region. Immunity 1999;11:567–578.
15. Doyonnas R, Nielsen JS, Chelliah S, et al. Podocalyxin is a CD34-related marker of murine hematopoietic stem cells and embryonic erythroid cells. Blood 2005;105:4170–4178.
16. Rump A, Morikawa Y, Tanaka M, et al. Binding of ovarian cancer antigen CA125/MUC16 to mesothelin mediates cell adhesion. J Biol Chem 2004;279:9190–9198.
17. Kreidberg JA, Sariola H, Loring JM, et al. WT-1 is required for early kidney development. Cell 1993;74:679–691.
18. Tanimizu N, Nishikawa M, Saito H, et al. Isolation of hepatoblasts based on the expression of Dlk/Pref-1. J Cell Sci 2003;116:1775–1786.
19. Tanaka M, Okabe M, Suzuki K, et al. Mouse hepatoblasts at distinct developmental stages are characterized by expression of EpCAM and DLK1: drastic change of EpCAM expression during liver development. Mech Dev 2009;126:665–676.
20. Suzuki K, Tanaka M, Watanabe N, et al. p75 Neurotrophin receptor is a marker for precursors of stellate cells and portal fibroblasts in mouse fetal liver. Gastroenterology 2008;135:270–281, e3.
21. Ijpenberg A, Perez-Pomares JM, Guadix JA, et al. Wt1 and retinoic acid signaling are essential for stellate cell development and liver morphogenesis. Dev Biol 2007;312:157–170.
22. Niederreither K, Subbarayan V, Dolle P, et al. Embryonic retinoic acid synthesis is essential for early mouse post-implantation development. Nat Genet 1999;21:444–448.
23. Perez-Pomares JM, Phelps A, Sedmerova M, et al. Experimental studies on the spatiotemporal expression of WT1 and RALDH2 in the embryonic avian heart: a model for the regulation of myocardial and valvuloseptal development by epicardially derived cells (EPDCs). Dev Biol 2002;247:307–326.
24. Asahina K, Tsai SY, Li P, et al. Mesenchymal origin of hepatic stellate cells, submesothelial cells, and perivascular mesenchymal cells during mouse liver development. Hepatology 2009;49:998–1011.
25. Kinoshita T, Sekiguchi T, Xu MJ, et al. Hepatic differentiation induced by oncostatin M attenuates fetal liver hematopoiesis. Proc Natl Acad Sci U S A 1999;96:7265–7270.

Received June 30, 2009. Accepted December 31, 2009.

Reprint requests
Address requests for reprints to: Atsushi Miyajima, PhD, Laboratory of Cell Growth and Differentiation, Institute of Molecular

and Cellular Biosciences, University of Tokyo, 1-1-1 Yayoi, Bunkyo-ku, Tokyo 113-0032, Japan. e-mail: miyajima@iam.u-tokyo.ac.jp; fax: (81) 3-5841-8475.

Acknowledgments

The authors thank Dr R. Nishinakamura and Dr S. Kawamata for providing us with $WT1^{+/-}$ mice and anti-ALCAM antibody, respectively, and Drs J. James, T. Itoh, N. Tanimizu, and H. Nonaka for valuable discussions and critical reading of the manuscript.

Transcript profiling (expression microarray): National Center for Biotechnology Information Gene Expression Omnibus accession no. GSE 18937. (http://www.ncbi.nlm.nih.gov/geo/query/acc.cgi?acc=GSE18937).

Conflicts of interest

The authors disclose no conflicts.

Funding

Supported in part by a research grant from the Ministry of Health, Labor and Welfare and Grant-in-Aid for Scientific Research and Global COE Project of the Ministry of Education, Culture, Sports, Science and Technology of Japan.

Supplementary Materials and Methods

Antibodies

Goat anti-mouse PCLP1 polyclonal Ab and rabbit anti-mouse Ki67 polyclonal Ab used for IHC were purchased from R&D Systems, Inc. Phycoerythrin-conjugated or biotinylated anti-mouse PCLP1 monoclonal Ab (clone 10B9) used for flow cytometry was supplied from Medical & Biological Laboratories, Co, Ltd (Nagoya, Japan). Biotinylated anti-mouse Msln monoclonal Ab (clone B35) for both IHC and flow cytometry was prepared as described previously.[1] Anti-mouse delta-like 1 homologue (Dlk1) monoclonal Ab[2] was biotinylated by ECL Protein Biotinylation Module (GE Healthcare, Tokyo, Japan) according to the manufacturer's protocol. Other fluorescently labeled Abs and anti-FcγR Ab used for flow cytometry were purchased from Pharmingen (San Diego, CA). To detect signals of biotinylated Abs in flow cytometry, allophycocyamin-conjugated streptavidin (BioLegend, San Diego, CA) was used.

IHC

Whole embryos or livers dissected from animals were frozen and cryosectioned into 6-μm slices. Sections were fixed with 4% paraformaldehyde in phosphate-buffered saline for 10 minutes at room temperature, followed by incubation with each primary Ab. Sections were incubated with fluorescently labeled secondary antibodies to detect signals by fluorescence microscopy. Ki67 immunocytochemistry was performed using PCLP1^{high} MCs sorted from E13.5 livers by a cell sorter. Cytospin samples were fixed and immunostained using Ki67 Ab as described previously.

Quantitative RT-PCR Analysis

Total RNA was extracted from cells by using TRIzol reagent (Invitrogen, Carlsbad, CA). First-strand complementary DNA was synthesized using a High Capacity cDNA Reverse Transcription Kit (Applied Biosystems, Foster City, CA) and was used as a template for PCR amplification. The primer sequences used are as follows: *GAPDH*, 5′-TGAACGGGAAGCTCACTGG-3′ and 5′-TCCACCACCCTGTTGCTGTA-3′; *Msln*, 5′-CTATCCTGAGTCCCTGATCCA-3′ and 5′-TCGCCTGAGCATTCATCTTT-3′; *HGF*, 5′-CCCGAGAACTTCAAATGCAA-3′ and 5′-TATGACGGTGTAAATCCTCCA-3′; *Ptn*, 5′-GGAAGAAGCAGTTTGGAGCTG-3′ and 5′-GGCGGTATTGAGGTCACATTC-3′; *Mdk*, 5′-TGATGGGAGCACTGGCAC-3′ and 5′-CATTGTACCGCGCCTTCTT-3′; *PCLP1*, 5′-GCAAGAGCGGTGACAGTTTTA-3′ and 5′-AGTTGTCAGTGCTGGGCGT-3′; *Msln*, 5′-CTATCCTGAGTCCCTGATCCA-3′ and 5′-TCGCCTGAGCATTCATCTTT-3′; *WT1*, 5′-CAGATGAACCTAGGAGCTACCTTAAA-3′ and 5′-CGTGGTTGCTCTGCCCTTCT-3′; *Raldh2*, 5′-CATGGTATCCTCCGCAATG-3′ and 5′-GCGCATTTAAGGCATTGTAAC-3′. The real-time PCR reactions were performed using LightCycler (Roche Diagnostics KK, Toyko, Japan) according to the manufacturer's protocol.

In Vitro Colony Formation Assay

MCs were prepared by sorting of Flk1^{-}PCLP1^{high} cells using EPICS ALTRA from E12.5 livers or by sorting of Msln^{+} cells using autoMACS or EPICS ALTRA from E18.5, PD7, or adult livers. MCs (1×10^3 cells) were then inoculated into each well of a type IV collagen-coated 6-well plate (AGC Techno Glass, Chiba, Japan) and cultured in α-minimum essential medium (Invitrogen) containing 10% fetal bovine serum (JRH Biosciences, Tokyo, Japan) and 50 nmol/L mercaptoethanol (Invitrogen). After 6 days of culture, the plates were stained with Giemsa solution (Merck, Damstadt, Germany) to visualize the cells and colonies were counted under the microscope. Averages of 3 wells from each sample were used to evaluate cell proliferation.

References

1. Rump A, Morikawa Y, Tanaka M, et al. Binding of ovarian cancer antigen CA125/MUC16 to mesothelin mediates cell adhesion. J Biol Chem 2004;279:9190–9198.
2. Tanaka M, Okabe M, Suzuki K, et al. Mouse hepatoblasts at distinct developmental stages are characterized by expression of EpCAM and DLK1: drastic change of EpCAM expression during liver development. Mech Dev 2009;126:665–676.

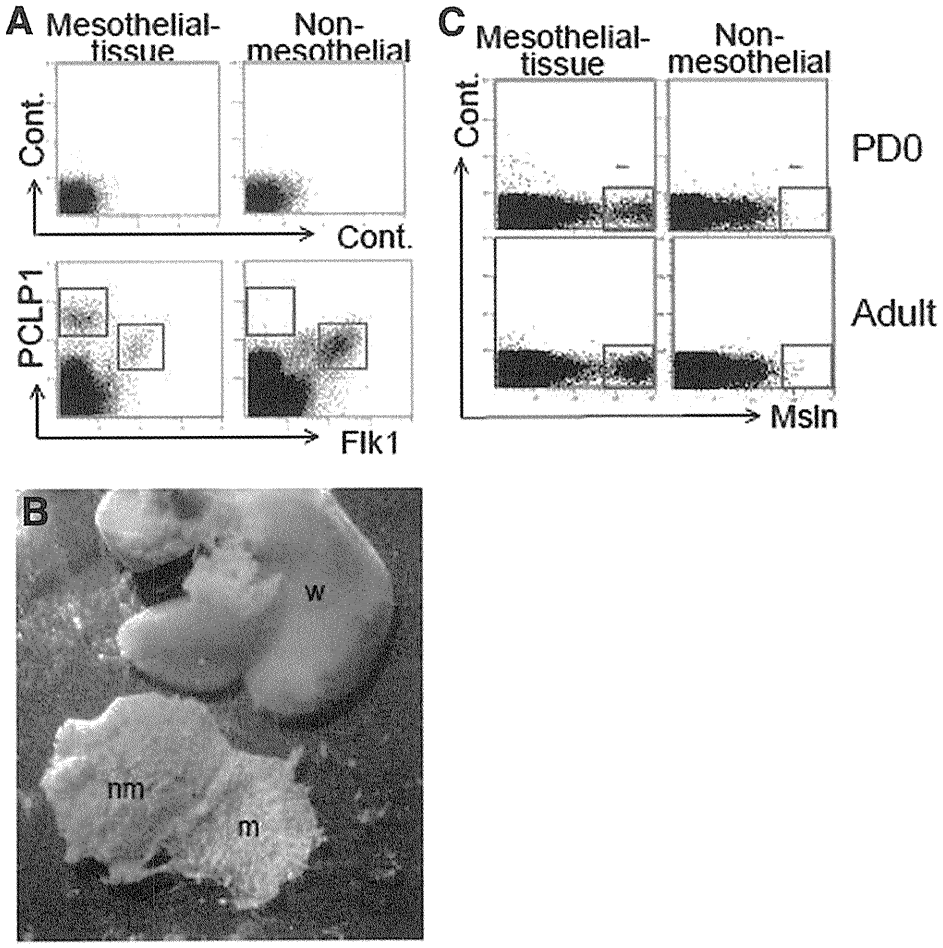

Supplementary Figure 1. (*A*) FCM of E16.5 liver cells with anti-PCLP1 and anti-Flk1 Abs. *Red* and *green lines* in *lower panels* indicate PCLP1^{high} and PCLP1^{med} cell populations, respectively. Note that Flk1^{-}PCLP1^{high} cells were present exclusively in the mesothelial tissue, while Flk1^{+}PCLP1^{med} cells were detected mainly in the non-mesothelial tissue. (*B*) Appearance of surgically separated adult liver mesothelial tissue (m) and non-mesothelial tissue (nm). w, non-separated whole liver. (*C*) FCM with anti-Msln Ab using neonatal (PD0) or adult liver cells. *Red lines* in each *panel* indicate Msln^{+} cell population. Note that the cells highly expressing Msln are exclusively detected in the surgically separated mesothelial tissue in PD0 and adult livers.

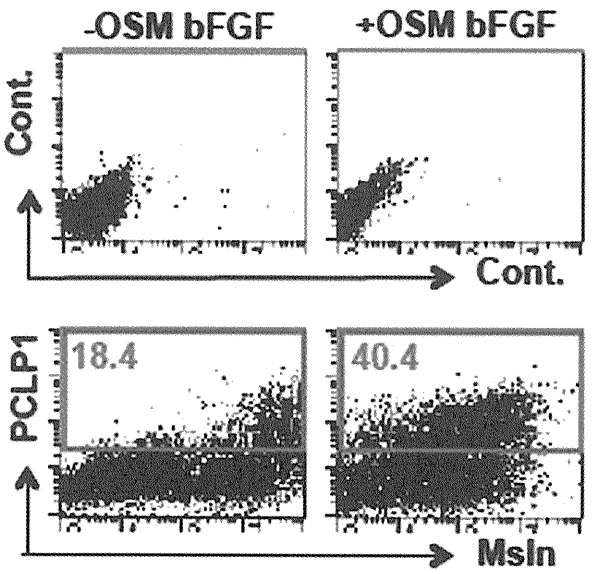

Supplementary Figure 2. FCM of cultured MCs with anti-PCLP1 and anti-MsIn Abs. After first passage of cultured E12.5 Flk1^{-}PCLP1^{high} cells in the presence of OSM and bFGF, the cells were incubated for additional 6 days in the presence or absence of the cytokines, followed by FCM. *Red lines* and numbers in *lower panels* indicate PCLP1^{+} cell populations and their percentages, respectively.

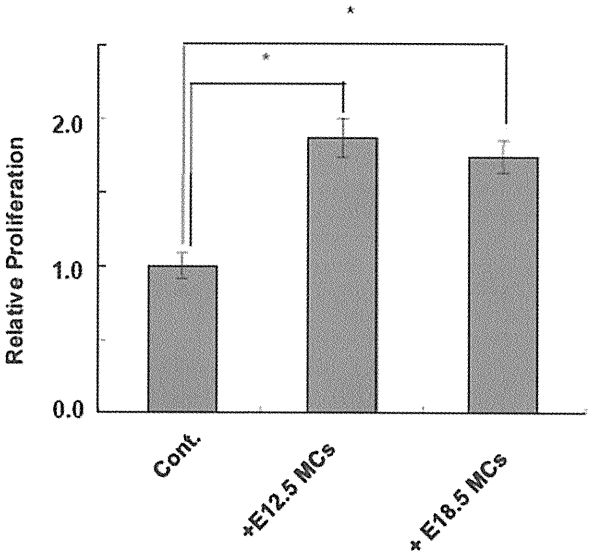

Supplementary Figure 3. Proliferation of E14.5 Dlk1^{+} cells cultured with in vitro expanded MCs from E12.5 or E18.5 livers. Growth of hepatocytes was measured by WST-1 assay after 3 days of coculture. Averages of 3 wells for each sample are shown. *$P < .005$; Student *t* test.

Supplementary Table 1. Growth Factors Preferentially Expressed in Immature MCs

Genbank	Gene symbol	Description	E12.5 PCLP1highMsIn^{-}	Adult MsIn^{+}	E12.5/Adult Ratio
AV240088	Fgf5	Fibroblast growth factor 5	413.0	1.0	>100.0
NM_010514	Igf2	Insulin-like growth factor 2	226.3	1.4	>100.0
BC002064	Ptn	Pleiotrophin	2129.3	18.1	80.0
U50279	Vegfa	Vascular endothelial growth factor A	79.7	0.8	68.3
AV269710	Angpt4	Angiopoietin 4	124.7	2.0	42.6
M34328	Mdk	Midkine	9680.6	158.6	41.5
AF020737	Fgf13	Fibroblast growth factor 13	198.8	4.1	32.9
NM_019971	Pdgfc	Platelet-derived growth factor, C polypeptide	2805.1	58.1	32.8
NM_008243	Mst1	Macrophage stimulating 1 (hepatocyte growth factor-like)	75.0	1.6	31.5
NM_010514	Igf2	Insulin-like growth factor 2	12,753.5	285.0	30.4
NM_019971	Pdgfc	Platelet-derived growth factor, C polypeptide	3830.3	109.1	23.9
BC002064	Ptn	Pleiotrophin	878.0	26.0	22.9
NM_009704	Areg	Amphiregulin	20.2	0.7	19.7
NM_009521	Wnt3	Wingless-related MMTV integration site 3	5.5	0.2	16.0
AU015375	Bmp15	Bone morphogenetic protein 15	12.7	0.6	15.5
NM_010201	Fgf14	Fibroblast growth factor 14	14.9	1.0	10.1
AV032115	Bmp5	Bone morphogenetic protein 5	133.8	9.6	9.4
AB073819	Wnt9b	Wingless-type MMTV integration site 9B	14.8	1.2	8.6
BB476818	Hgf	Hepatocyte growth factor	143.2	12.9	7.5
AB016516	Fgf5	Fibroblast growth factor 5	26.6	2.5	7.3
AK003506	Il17b	Interleukin 17B	35.1	3.6	6.6
NM_009505	Vegfa	Vascular endothelial growth factor A	660.0	75.6	5.9
NM_021782	Il21	Interleukin 21	15.7	1.9	5.6
NM_021380	Il20	Interleukin 20	67.4	8.8	5.2
BM210179	Bmp8b	Bone morphogenetic protein 8b	22.9	3.0	5.2

NOTE. Microarray analysis was performed using E12.5 PCLP1^{high}MsIn^{-} immature MCs and adult mature MsIn^{+} MCs. The list shows growth factors whose expression in E12.5 MCs is more than 5 times higher than adult MCs.

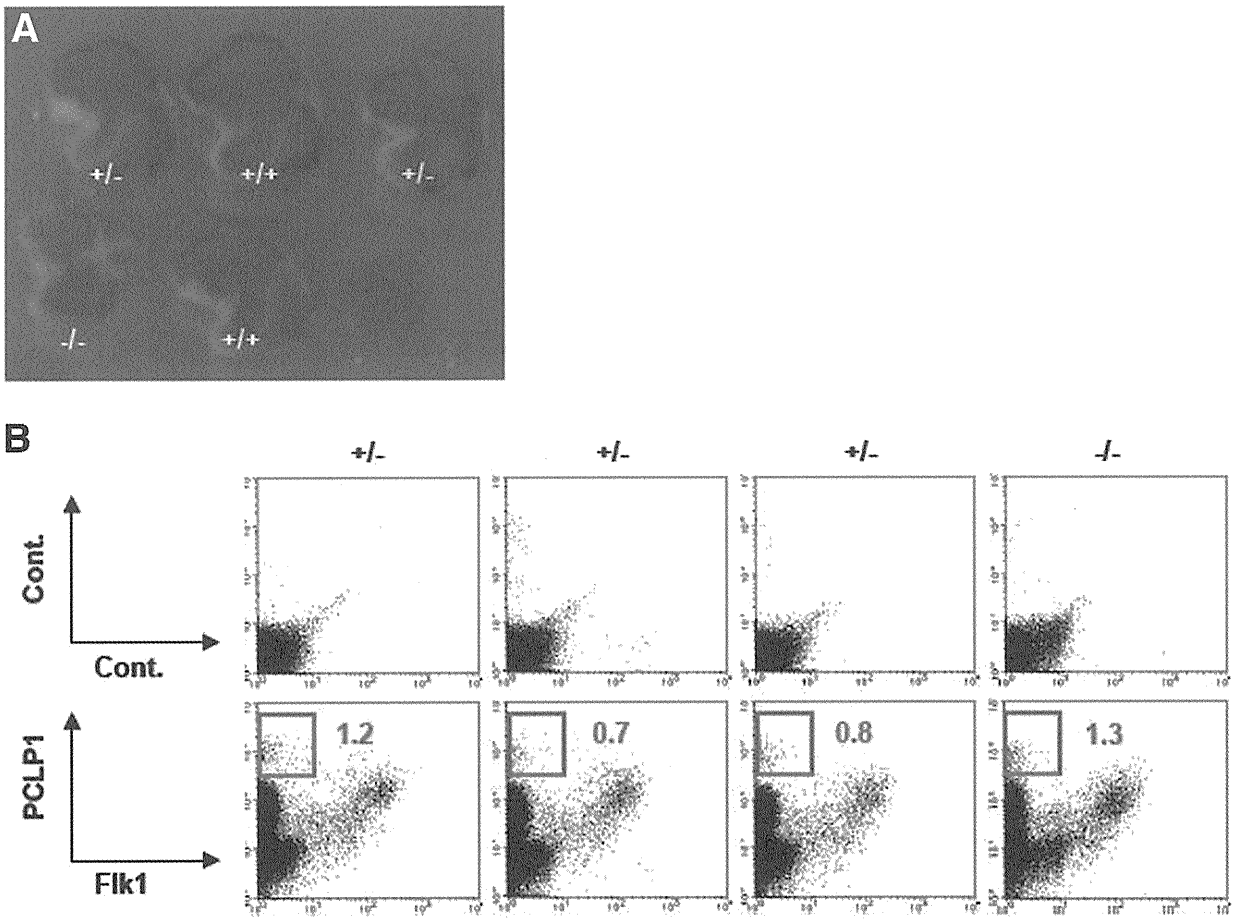

Supplementary Figure 4. (*A*) The morphology of E13.5 livers from littermates with each genotype. Note that the liver of $WT1^{-/-}$ embryo is smaller than those of the other littermates. (*B*) FCM of E13.5 liver cells from each littermate with anti-Flk1 and anti-PCLP1 Abs. The genotypes are indicated above each *panel*. *Red lines* and numbers in the *lower panels* indicate $Flk\text{-}1^{-}PCLP1^{high}$ cells and its percentages, respectively. Note that $Flk1^{-}PCLP1^{high}$ cells are detected in $WT1^{-/-}$ FLs as well as $WT1^{+/-}$ littermates.

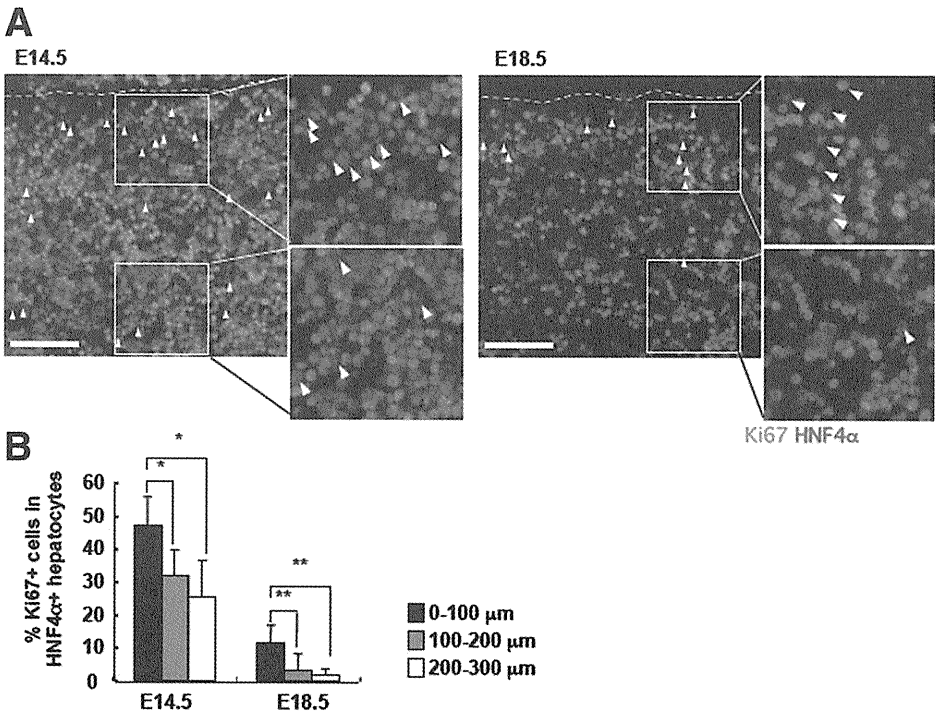

Supplementary Figure 5. Distribution of proliferating hepatocytes in the developing liver (*A*) immunostaining of E12.5 and E18.5 FL sections with anti-Ki67 (*green*) and anti-HNF4α (*red*) Abs. The *dotted lines* in the *left panels* indicate MC layer. Higher magnified images of *boxed areas* are shown in the *right*. The *arrowheads* indicate Ki67+HNF4α+ cells. Note that Ki67$^+$HNF4α^+ cells are observed more abundantly in the peripheral regions than in the central regions of hepatic lobes. *Scale bars*, 80 μm. (*B*) The percentages of Ki67$^+$ cells in HNF4α^+ cells in each 100 × 300 μm^2 area at 0–100, 100–200, and 200–300 μm distance from the MC layer. Microscopic views of 300 μm × 300 μm were used for analyses (E14.5, n = 5; E18.5, n = 12). *$P < .05$; **$P < .005$; Student *t* test.

Supplementary Table 2. The Number of HNF4α^+ cells Used for Analysis

	Number of HNF4α^+ cell in each 100 × 300 μm^2 area		
	0–100 μm	100–200 μm	200–300 μm
E14.5 (n* = 5)	38.4 ± 8.3 (47.2 ± 8.7)	38.8 ± 9.5 (32.1 ± 8.0)	35.2 ± 5.0 (25.4 ± 11.3)
E18.5 (n* = 12)	56.9 ± 10.9 (11.5 ± 5.4)	58.4 ± 7.0 (3.2 ± 5.0)	52.9 ± 8.0 (1.7 ± 2.0)

NOTE. The number of HNF4α^+ cells in each 100 × 300 μm^2 area at 0–100, 100–200, and 200–300 μm distance from the MC layer was counted for Supplementary Figure 4*B*. The percentages of Ki67$^+$ cells in HNF4α^+ cells are shown in parentheses. n*, number of 300 μm × 300 μm views.

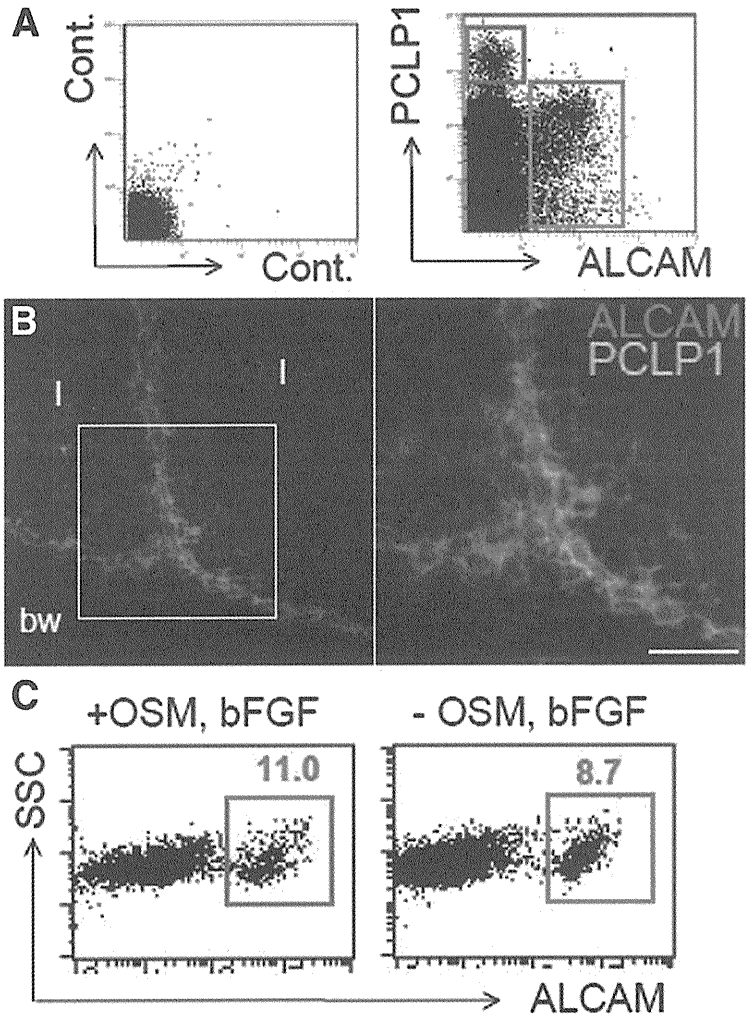

Supplementary Figure 6. (*A*) FCM of E12.5 liver cells using fluorescently labeled Abs against ALCAM and PCLP1. *Red* and *green lines* in the *right panel* indicate PCLP1^{high} cells and ALCAM^{+} cells, respectively. Note that PCLP1^{high} cells are negative for ALCAM. (*B*) IHC on E13.5 liver sections with anti-ALCAM (*red*) and anti-PCLP1 (*green*) Abs. Higher magnification image of the *boxed region* in the *left panel* is shown in the *right panel*. Note that PCLP1^{+} MC layers and ALCAM^{+} submesothelial layers are clearly distinguishable. l, lobe; bw, body wall. *Scale bar*, 40 μm. (*C*) FCM of cultured MCs using fluorescently labeled Abs against ALCAM. PCLP1^{high} cells sorted from E12.5 FL were cultured in the presence of OSM and bFGF, and further cultured for 3 days in the presence or absence of OSM and bFGF. Note that ALCAM^{-}PCLP1^{high} immature MCs give rise to ALCAM^{+} cells in vitro.

IκBη, a nuclear IκB protein, positively regulates the NF-κB–mediated expression of proinflammatory cytokines

Shumpei Yamauchi, Hiroaki Ito[1], and Atsushi Miyajima[2]

Laboratory of Cell Growth and Differentiation, Institute of Molecular and Cellular Bioscience, University of Tokyo, Bunkyo-ku, Tokyo 113-0032, Japan

Edited by Shizuo Akira, Osaka University, Osaka, Japan, and approved May 26, 2010 (received for review November 17, 2009)

NF-κB is a key mediator for inducible transcription of various proinflammatory genes in innate immune responses, and its activity is strictly regulated by several IκB proteins. Although signaling pathways leading from pattern recognition receptors to NF-κB's activation in the cytoplasm have been studied extensively, the detail regulatory mechanisms of NF-κB–mediated transcriptional activity in the nucleus still remain unclear. Here we describe a unique member of the nuclear IκB protein family, IκBη. In a gene expression analysis of dendritic cells, we found a unique gene encoding an uncharacterized protein with ankyrin repeats. As it was structurally related to the IκB family, the protein was named "IκBη" and further characterized in the innate immune response. IκBη was widely expressed in various tissues and predominantly located in the nucleus. Moreover, biochemical analysis showed that IκBη associated with the p50 subunit of NF-κB. Knockdown of IκBη by siRNA suppressed the transcription of a subset of NF-κB–mediated proinflammatory cytokines in LPS-stimulated and poly (I:C)-transfected macrophages. These results indicate that IκBη regulates the NF-κB–mediated transcription of a wide variety of proinflammatory genes, playing a crucial role in the regulation of innate immune responses.

innate immunity | Toll-like receptor | macrophage | signal transduction | ankyrin repeat

The NF-κB/Rel family, consisting of p50 (NF-κB1), p52 (NF-κB2), p65 (RelA), RELB, and REL (c-Rel), play a central role in the regulation of inducible gene expression in various biological systems (1–3). In response to stimuli, a dimer of NF-κB proteins binds to a κB site in the promoter or enhancer of a target gene, resulting in the expression of various inflammatory genes. The signaling pathways of NF-κB have been characterized extensively in innate immune responses. Pattern recognition receptors (PRRs), such as Toll-like receptors (TLRs), recognize microbial components or viral nucleic acids and activate the NF-κB signal-transduction pathway to induce expression of a wide variety of inflammatory gene products, such as TNF-α, IL-6, and IFNs, playing a key role in innate immune responses (4).

NF-κB proteins are constitutively expressed in unstimulated cells, but their activities are strictly repressed by an inhibitor of NF-κB (IκB) protein (1, 5). Seven IκB proteins have been identified to date: IκBα, IκBβ, IκBε, IκBγ, BCL-3, IκBNS, and IκBζ. These proteins are characterized by multiple ankyrin repeats and interaction with an NF-κB subunit. In unstimulated cells, NF-κB forms an inert complex with a canonical IκB protein, such as IκBα or IκBβ, which masks the nuclear localization signal of NF-κB and sequesters the complex away from the nucleus. To activate NF-κB's transcriptional activity, the IκB protein needs to be released from the NF-κB/IκB complex (3). Upon stimulation, TLRs activate IκB kinase via a protein cascade, leading to phosphorylation of IκB bound to NF-κB. Phosphorylated IκB proteins were degraded by the proteasome system, releasing NF-κB from the inactive complex with canonical IκB proteins. Free NF-κB translocates into the nucleus and regulates transcription of target genes by binding to κB sites in their promoters or enhancers.

A wide variety of proinflammatory genes are regulated by NF-κB, and its regulatory mechanisms are also diverse because of cooperating with multiple regulatory factors. In addition to the canonical IκB proteins acting as inhibitors of NF-κB signal transduction in the cytoplasm, there are nuclear IκB proteins, such as BCL-3, IκBNS, and IκBζ, which are present in the nucleus and thought to regulate the transcriptional activity of NF-κB (5, 6). Although less expressed under normal conditions, these nuclear IκB proteins are highly inducible in response to stimuli. BCL-3 functions as either an activator or an inhibitor of NF-κB in a context-specific manner by regulating its transcriptional activity or its stability on DNA (7, 8). IκBNS inhibits IL-6 production by associating with DNA-bound p50 homodimers, preventing the binding of NF-κB dimers to the promoters (9, 10). IκBζ induced to express by stimuli binds to p50 on IL-6 and IL-12p40 promoters, and is supposed to activate transcription by remodeling the nucleosomes in targeted regions (11, 12). Therefore, the transcriptional activity of NF-κB is regulated not only by cytoplasmic IκBs, but also by nuclear IκBs, to strictly modulate the NF-κB–mediated expression of inflammatory genes. However, factors regulating NF-κB's activity in the nucleus still remain largely unknown.

In this article, we describe a unique molecule with ankyrin repeats that was found in a gene expression analysis of bone marrow-derived dendritic cells (BMDCs). Because it is structurally related to the IκB family, we have named the protein "IκBη" and further studied its expression and functions, especially in innate immune responses. We found that IκBη is predominantly located in the nucleus and interacts with the p50 subunit of NF-κB. We also showed that IκBη modulates the NF-κB–mediated transcriptional activity for the expression of a subset of proinflammatory genes. Based on these results, we propose that IκBη is a unique nuclear IκB protein playing a crucial role for regulating the expression of proinflammatory genes in innate immune responses.

Results

IκBη Is a Unique Member of the IκB Family. To find novel molecules involved in the regulation of immune responses, a microarray analysis was performed using mRNA from mouse BMDCs. Among many genes expressed in BMDCs, we were interested in one gene encoding ankyrin repeats, because ankyrin repeats are known to be important for interaction with NF-κB, a central regulator of inflammation (13). This gene was identical to the

Author contributions: S.Y., H.I., and A.M. designed research; S.Y. and H.I. performed research; S.Y. and H.I. contributed new reagents/analytic tools; S.Y. and A.M. analyzed data; and S.Y. and A.M. wrote the paper.

The authors declare no conflict of interest.

This article is a PNAS Direct Submission.

[1]Present address: Immunology Program, Benaroya Research Institute at Virginia Mason, 1201 9th Avenue, Seattle, WA 98101.

[2]To whom correspondence should be addressed: E-mail: miyajima@iam.u-tokyo.ac.jp.

This article contains supporting information online at www.pnas.org/lookup/suppl/doi:10.1073/pnas.0913179107/-/DCSupplemental.

Ankrd42 gene in databases, but its function had not been described. The protein encoded by the gene consists of 516 amino acid residues and has eight ankyrin repeats in the NH_2-terminal region and a coiled-coil domain in the COOH-terminal region (Fig. 1*A*). Its amino acid sequence, especially the ankyrin-repeats domain, is highly conserved in mouse, rat, and human, and closely related to that of the IκB family, well-known regulators of NF-κB signal transduction (Fig. 1*B* and Fig. S1*A*). Moreover, the protein was similar in function to IκB proteins as described below. Therefore, we have named it IκBη and further analyzed its expression and functions.

The tissue distribution of IκBη in adult mice was examined by Northern blotting (Fig. 1*B*). An ≈2.8-kb mRNA for IκBη was rather ubiquitously expressed in all of the tissues examined and highly expressed in the brain, lung, testis, and ovary. As NF-κB mediates a central signaling pathway in innate immune responses and IκB family proteins are major components of NF-κB signal transduction, we examined the expression of IκBη in antigen-presenting cells by RT-PCR assay and revealed that IκBη was expressed not only in dendritic cells but also in macrophages in the spleen (Fig. S1*B*). IκBη was also expressed in T cells and B cells (Fig. S1*B*). These results indicate that IκBη is ubiquitously expressed in various tissues and blood cells, including antigen-presenting cells.

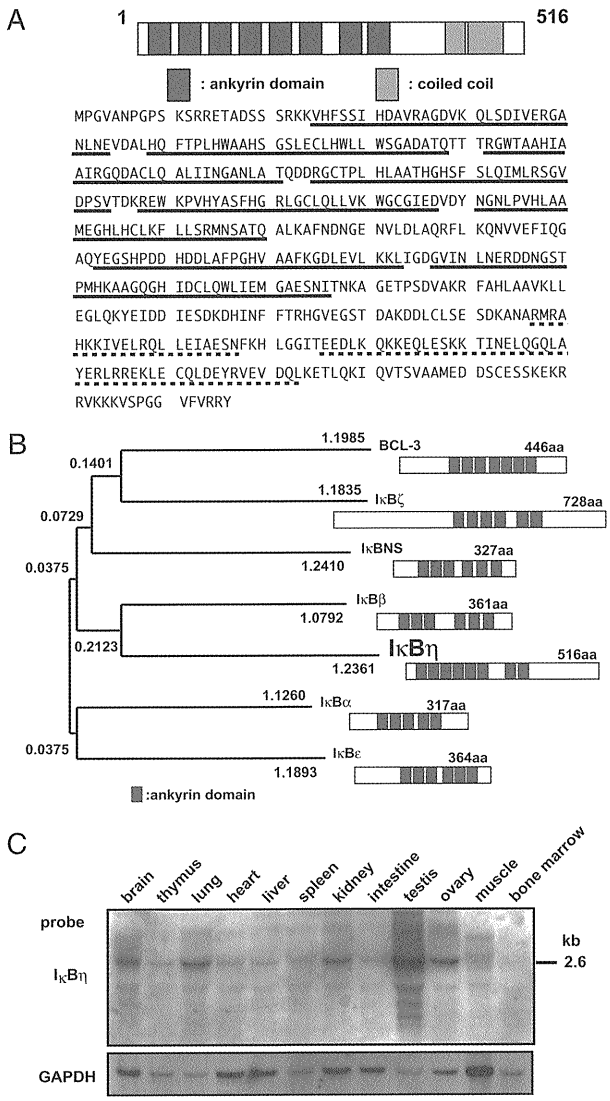

Fig. 1. Structure and tissue distribution of mouse IκBη. (*A*) The amino acid sequence and a structural diagram of IκBη. The ankyrin repeats and coiled-coil domains are indicated by blocks and boxes, respectively. Black underlines indicate ankyrin domains and the dotted underline indicates the putative coiled-coil region. (*B*) A phylogenic tree of mouse IκB family proteins, obtained using the Neighbor-Joining method. Diagrams of each IκB protein and ankyrin domains are shown on the right. (*C*) Northern blot of mouse tissues probed with mouse IκBη or the GAPDH control probe. Each lane contains 20 μg of total RNA. The position of the 2.6 kb marker is indicated.

Expression and Subcellular Distribution of IκBη. Because the expression of IκB proteins is known to be highly inducible, we examined whether the expression of IκBη was regulated by TLR signals by real-time RT-PCR (Fig. 2*A*). Expression of *Ikbh* mRNA in the macrophage cell line Raw264.7 was constitutive and only slightly up-regulated by LPS. In addition to LPS, zymosan, poly (I:C) and CpG DNA, ligands for TLR2, TLR3, and TLR9, respectively, also only marginally increased the expression of IκBη in Raw264.7 cells (Fig. 2*A*). The induction was

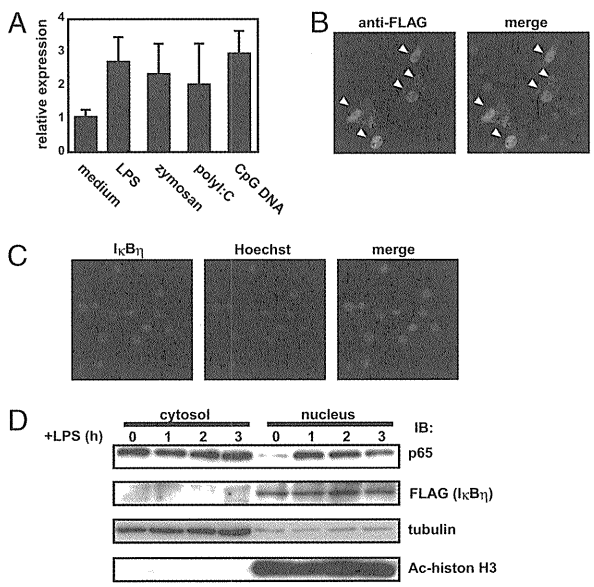

Fig. 2. Expression and subcellular distribution of IκBη. (*A*) Raw264.7 cells were treated with medium, LPS (100 ng/mL), zymosan (1 mg/mL), poly (I:C) (25 μg/mL), and CpG DNA (1 μM) for 90 min and the expression of *Ikbh* and *Hprt* mRNA was measured by real-time RT-PCR. The expression of IκBη was normalized to that of the housekeeping gene *Hprt*. The data are shown as the relative expression of *Ikbh* compared with untreated cells. (*B*) NIH 3T3 cells were transfected with FLAG-tagged IκBη for 24 h. Cells were stained with anti-FLAG Ab (green) as well as Hoechst dye (blue), and analyzed by microscopy. Arrowheads indicate transfected cells. (*C*) NIH 3T3 cells were stained with anti-IκBη Ab (green) as well as Hoechst dye (blue), and analyzed by microscopy. (*D*) Raw264.7 cells were transiently transfected with FLAG-tagged IκBη and then stimulated with LPS. Cytoplasmic and nuclear fractions were isolated and subjected to Western blotting using anti-IκBα, anti-p65, anti-FLAG Abs. Tubulin and acetyl-histone H3 were used as a cytoplasmic and nuclear marker, respectively. Data shown are representative of two or three experiments.